Wodebo, Desta Yoseph; Melesse, Assefa M.; Woldesenbet, Tekalegn Ayele; Mekonnen, Kirubel; Amdihun, Ahmed; Korecha, Diriba; Tedla, Hailay Zeray; Corzo, Gerald; Teshome, Asaminew

Comprehensive performance evaluation of satellite-based and reanalysis rainfall estimate products in Ethiopia : For drought, flood, and water resources applications

Published in:
Journal of Hydrology: Regional Studies

DOI:
10.1016/j.ejrh.2024.102150

Published: 01/02/2025

Document Version
Publisher's PDF, also known as Version of record

Please cite the original version:
Wodebo, D. Y., Melesse, A. M., Woldesenbet, T. A., Mekonnen, K., Amdihun, A., Korecha, D., Tedla, H. Z., Corzo, G., & Teshome, A. (2025). Comprehensive performance evaluation of satellite-based and reanalysis rainfall estimate products in Ethiopia : For drought, flood, and water resources applications. *Journal of Hydrology: Regional Studies*, *57*, Article 102150. https://doi.org/10.1016/j.ejrh.2024.102150

Journal of Hydrology: Regional Studies 57 (2025) 102150

Contents lists available at ScienceDirect

Journal of Hydrology: Regional Studies

journal homepage: www.elsevier.com/locate/ejrh

Comprehensive performance evaluation of satellite-based and reanalysis rainfall estimate products in Ethiopia: For drought, flood, and water resources applications.

Desta Yoseph Wodebo [a,*], Assefa M Melesse [b], Tekalegn Ayele Woldesenbet [a], Kirubel Mekonnen [c], Ahmed Amdihun [d], Diriba Korecha [e], Hailay Zeray Tedla [f], Gerald Corzo [g], Asaminew Teshome [h]

[a] Ethiopian Institute of Water Resources, Addis Ababa University, Addis Ababa, Ethiopia
[b] Department of Earth and Environment, Institute of Environment, Florida International University, Miami, USA
[c] International Water Management Institute, Addis Ababa P.O. Box 5689, Ethiopia
[d] IGAD Climate Prediction and Applications Centre, Nairobi P.O. BOX 10304 -00100, Kenya
[e] University of California Santa Barbara, Climate Hazards Center, Famine Early Warning Systems Network, Addis Ababa P.O. Box 17483, Ethiopia
[f] Water and Environmental Engineering, Department of Built Environment, Aalto University, Aalto, Finland
[g] Hydroinformatics Department, IHE Delft Institute for Water Education, Westvest 7, Delft 2611 AX, Netherlands
[h] Ethiopian Meteorological Institute, Addis Ababa P.O. BOX 1090, Ethiopia

ARTICLE INFO

Keywords:
Satellite and reanalysis rainfall products
Validation
Applications
Flood
Drought
Water resources
Ethiopia

ABSTRACT

Study Region Ethiopia: This study assessed the accuracy of ten satellite-based and reanalysis rainfall estimation products across Ethiopia via direct comparisons with 430 in-situ datasets from 2001 to 2020. The performance of these rainfall products at various spatial and temporal scales was validated via five continuous and six categorical metrics to identify the most reliable products for the application of drought monitoring, flood risk analysis, and water resources management in 92 zonal administrative and 76 subbasins boundaries in Ethiopia.

New hydrological insights for the region: This study revealed that the performance of rainfall products varies over space and time and is heavily impacted by the diverse climate and topography of Ethiopia. In general: ARCv2.0 and CHIRPSv2.0 detected rainfall of less than 1 mm and well-captured drought-year monthly products, making them suitable for drought monitoring. The IMERG-Fv6B and TAMSATv3.1 products were found to be reliable for detecting heavy rainfall and suggested for flood monitoring. Similarly, for water resources potential studies, CHIRPSv2.0 and MSWEPv2.8 were identified as reliable products at all 50 spatial scales of the analysis. This study offers multiple novel perspectives for selecting location-specific suitable rainfall products as decision-support information for water resources, flood risk management, and drought monitoring in Ethiopia. The findings also imply the importance of bias correction or blending of satellite data for a better representation of the true value.

* Corresponding author.
E-mail address: destayoseph@gmail.com (D.Y. Wodebo).

https://doi.org/10.1016/j.ejrh.2024.102150
Received 12 August 2024; Received in revised form 20 December 2024; Accepted 22 December 2024
Available online 3 January 2025

1. Introduction

Accurate and representative rainfall information is crucial for Ethiopia, as its economy relies heavily on rainfall-sensitive sectors, such as agriculture and water resources (Borgomeo et al., 2018; Yalew, 2022). The agricultural output and economic growth of the country are closely linked to rainfall (World Bank 2006), and approximately 85 % of the Ethiopian labour force is deployed in a rainfed agricultural system (Alhamshry et al., 2020). Rainfall determines water resource availability and related productivity. For example, hydropower production in Ethiopia accounts for 90 % of the current energy production share (Yalew, 2022). In addition to its economic significance, variability in rainfall is viewed as a threat to development by causing recurrent droughts and flooding (World Bank, 2019). Hence, representative rainfall information is vital for making informed decisions in Ethiopia, where the economy depends heavily on rainfall.

Conventional meteorological gauges are commonly used as reliable rainfall data sources (Teixeira de Aguiar and Lobo, 2020). However, spatiotemporal inadequacy (Dinku, Funk, Peterson, Maidment, and Tadesse, 2018), the decline of real-time gauge records in some parts of the country (Dinku, 2019), and the dominance of rainfall measuring gauges in urban areas (NMA, 2021) sometimes compromise the representativeness of gauge data as the only source. According to the revised Meteorological Station Network Master Plan of Ethiopia (Ababa, 2021), lowland areas of the country require a significant number of additional weather stations to fulfil the WMO standards, which is one station for 100–250 km^2 (WMO, 2012). Furthermore, data-access policies sometimes make users pay, or they may require a time-consuming process to acquire. All these factors can be considered the main challenges to relying only on meteorological stations, and it is important to consider open-source, but reliable satellite-based rainfall estimates and reanalysis data as complementary sources of rainfall information.

Satellite-based Rainfall Estimates (SbRE) and reanalysis rainfall products have become increasingly complementary and promising alternative sources of ground weather station rainfall data for supporting decisions in various sectors. For example, it has been used for general water resource studies (Dumont et al., 2022; Filippucci et al., 2022; Getirana et al., 2011; Sheffield et al., 2018; Wei et al., 2023), dam design and simulation (Bertini et al., 2020; Bonnema et al., 2016; Prakoso et al., 2018; Velpuri et al., 2016), agriculture and food security (Gummadi et al., 2022; Omondi et al., 2021; Xia et al., 2018), flood risk management and forecasting (Bajracharya et al., n.d.; Hinge et al., 2022; Matingo et al., 2018; Moura et al., 2022; Yoshimot and Amarnath, 2017), and drought analysis (Katiraie-Boroujerdy et al., 2016; Lemma et al., 2022; Nile and Bayissa, 2017; Taye et al., 2020; F. Wang et al., 2019).

The performance of SbRE is highly altered by various factors, including the topographic gradient (Gebremicael et al., 2017; Mohammed et al., 2020; Tang et al., 2023; Thakur et al., 2019), spatiotemporal scale (Zambrano-bigiarini et al., 2017), climatic situation (Mekonnen et al., 2023), length of data used for evaluation (Abera et al., 2016), ground observation density (Macharia et al., 2022), resolution (Vergara et al., 2014) and sensors used for SbRE development (Mekonnen et al., 2021). For example, Zambrano-bigiarini et al. (2017) conducted a national-scale evaluation for Chile in the diverse climate and complex topography of Chile on daily, monthly, seasonal, and annual scales considering the SbRE products of CHIRPSv2, PERSIANN-CDR, PERSIAN-CCS-Adj, TMPA 3B42v7, CMORPH, PGFv3, and MSWEPv1.1. They reported that the overall performance skills of MSWEPv1.1, CHIRPSv2, and TMPA 3B42v7 are better than those of the other three SbRE products. All SbRE products performed better in wet (autumn and winter) seasons than in the other two seasons (DJF and summer and SON or spring seasons), and most SbRE products performed better in low- and mid-elevation (0–1000 m.a.s.l.) areas than in arid northern and far southern China. The results indicate that the performance of SbRE within a country is heavily impacted by the temporal resolution of SbRE, topography, and climate patterns.

Ethiopia is among the leading countries in Africa, where multiple SbRE evaluation or validation studies have been conducted to quantify systematic and random errors and choose suitable SbRE products (Ali et al., 2023). However, SbRE or reanalysis validation studies have been conducted in a fragmented manner, with a focus on the river basin, subbasin, or catchment scale (Table 1) or concentrated in a certain area, such as upstream of the Abay River Basin (Alghafli et al., 2023; Almaw et al., 2018; Bitew and Gebremichael, 2011; Cha et al., 2014; Tadesse et al., 2022; Gebremichael et al., 2014) and Awash River Basin (Adane, Hirpa, Gebru, et al., 2021; Adane, Hirpa, Lim, et al., 2021; Asfaw et al., 2023), where a comprehensive evaluation of SbRE is often missing. Country-scale studies have been conducted during the early generation stage of SbRE products using a limited number of ground observations (Romilly and Gebremichael, 2011) and have not covered a significant portion of the country (Young et al., 2014). Ethiopia is renowned for its diverse topography (Faccenna et al., 2019), which is expected to impact the behaviour of SbRE products (Gebere et al., 2015); however, the topographic impact on the representativeness of SbRE and reanalysis products remains unknown. The performance of gauge-corrected products is likely hindered by the uneven distribution of ground measurement gauges, particularly in the less populated parts of the southern and eastern regions of Ethiopia. Furthermore, most previous validation studies considered short period time series of in-situ data and few SbRE products (Table 1). The various factors mentioned above may limit the accuracy and reliability of the SbRE and reanalysis products. Hence, it is essential to validate SbRE and analyse rainfall estimation products against ground-based rain gauge measurements to ensure the representativeness and reliability of rainfall products for various applications.

Pixel-to-point and pixel-to-pixel methods are two common approaches usually applied for SbRE validation: the former is recommended for locations with sparse station distributions (Dinku, Funk, Peterson, Maidment, and Tadesse, 2018; Mekonnen et al., 2023), and the latter is used for properly gauged areas that presumably fulfil WMO station distribution standards (Liu et al., 2019; Palharini et al., 2020). Owing to the uneven distribution of ground observation stations across Ethiopia, it is more appropriate to utilize the pixel-to-point approach when evaluating SbRE data in the context of Ethiopia.

This study focuses on validating ten SbRE and reanalysis of rainfall estimate products over Ethiopia from 2001 to 2020. The goal of this study was to understand the comprehensive performance of SbRE at different spatial and temporal scales. Spatial validation encompasses an understanding of the impact of different classification approaches on the choice of best-performing rainfall products,

Table 1
Some of the previous SbRE validation studies were conducted at regional, national, subnational, basin, subbasin, or catchment scale across the Ethiopian River Basin.

S. No	Spatial extent	Subspatial extent description	Temporal extent	Number of SbRE products and names	number of years, study period	Major findings	Study source
1	Regional, National	East Africa and Ethiopia (north and south of the Rift Valley; northwest (NW) and Southeast (SE) of Ethiopia)	Daily, monthly	4products (CHIRP, CHIRPS, ARC2 and TAMSAT3)	5 years (2006–2010)	On a daily base, correlation is low over both NW and SE parts of Ethiopia, but the overall performance of all products in NW>SE. Monthly, the performance of CHIRPS and CHIRP products is significantly better than TAMSAT3 and followed by ARC2	(Dinku, Funk, Peterson, Maidment, Tadesse, et al., 2018)
2	National	Ethiopia and 6 river basins (Blue Nile, Awash, Baro Akobo, Wabi Shebele, Rift Vally, and Genale Dawa)	3 hr	3 products (CMORPH, PERSIANN, TMPA 3B42RT)	5 years (2003–2007)	Microwave-based products (TMPA 3B42RT and CMORPH) outperform infrared-based products (PERSIANN). TMPA3B42RT and CMORPH performed better in the highland, and PERSIANN performed better in the lowland. All three products were underestimated in the Wabishebele & Genale Dawa Basins (lowland)	(Romilly and Gebremichael, 2011)
3	Sub National	Central Ethiopian highlands (Oromia Regional state)	3 hr daily	2 products(TRMM 3B42 and CMORPH) 2 products (TAMSAT and ARC)	14 years (1998–2012) 29 years (1983–2012)	TAMSAT was good at detecting rainy events but underestimated the amount; ARC underestimated both the amount and frequency. TRMM is best in capturing mean value, CMORPH over detected rain events.	(Young et al., 2014)
4	Basin	Awash (by dividing into 6 subbasins)	Monthly	4products (IMERGv06, TRMM−3B43v7, PERSIANN-CDR, GSMap-NRT)	17 years (1998–2014)	All products showed relatively lower detection skills in the western highland and good skills in the upper highland (PERSIANN-CDR best). IMERGv06 better performed across the entire basin.	(Adane, Hirpa, Lim, et al., 2021)
5	Subbasin	Awash (upper Awash highland vs Lowland; Microwave, MW-based rainfall data vs Infrared, IR-based rainfall data)	daily	7 products: MW (CMORPHv1, TRMM−3B42RT, TRMM 3B42v7 and IMERG-v06B) and IR (PERSIANN, PERSIANN-CDR and TAMSATv3)	12 years (2003–2015)	IMERG-v06B is best in the highland and TAMSATv3 in the lowland. TAMSATv3 is best at detecting low rates both in highlands and lowlands. IMERG-v06B underestimates high rainfall rates. MW and IR products detect better high and low rainfall rates in highland and lowland parts, respectively.	(Mekonnen et al., 2021)
6	Basin	Abay or upper Blue Nile Basin	Dekadal monthly	4products (CHIRPSv2.0, TAMSATv3, TAMSATv2, ARC 2)	16 years (2000–2015)	The best, in performance order in both dekadal and monthly scales was CHIRPS, TAMSAT 3, and ARC 2.	(Ayehu et al., 2018)
7	Subbasin	Abay or Blue Nile (lowland vs highland)	3 hr	3 products (CMORPH, TMPA-RP, TMPA-RT)	2years summer months (June-September) 2012&2013	All products overestimate the mean rainfall rate at the lowland plain and underestimate it at the highland mountain site. CMORPH's large positive bias at the lowland plain. TMPA-RT and TMPA-RP do not well detect a significant number of rainy cases.	(Cha et al., 2014)
8	Sub Basin	Abay or Blue Nile	daily	5products (CMORPH, TRMM, TMPA−3B42v7, ERAI, GPCC, MSWEP)	13 years (2000–2012)	MSWEP performed better than the other four products.	(Lakew et al., 2020)
9	Basin	Wabi Shebelle	Daily Monthly	3(CHIRPSv2, PERSIANN-CDR, TAMSATv3)	31 years (1983–2014)	For daily, in order performance, TAMSATv3 >PERSIANN-CDR> CHIRPSv2; but in monthly base, the order of performance was CHIRPSv2 >TAMSATv3 > PERSIANN-CDR.	(Tadesse et al., 2022)
10	Basin	Omo Gibe	Monthly Seasonal annual	4 products (CHIRPS, PERSIANN-CCS, PERSIANN, TAMPA)	20 years (2000–2019)	In all temporal scales, the order of performance was CHIRPS> PERSIANN-CCS> TMPA> PERSIANN.	(Dejene et al., 2023)

(continued on next page)

Table 1 (*continued*)

S. No	Spatial extent	Subspatial extent description	Temporal extent	Number of SbRE products and names	number of years, study period	Major findings	Study source
11	Basin	Baro Akobo	daily	5 products (CMORPH, TRMM−3B42, RFE2.0, PERSIANN, ERA-Interim)	5 years (2003–2008)	CMORPH performed better than all other products.	(Thiemig et al., 2013)
12	Subbasin	Rift Valley Lakes (Ziway Lake Basin)	Monthly, seasonal	2 products (GPM-IMERG and CHIRPS)	15 years (2000–2014)	CHIRPS slightly outperformed GPM-IMERG both on monthly and seasonal scales.	(Hordofa et al., 2021)
13	Subbasin	Tekeze-Atbara Basin	daily, monthly, and seasonal	8 products (CHIRPS, TRMM, CMAP, RFEv2, ARC2, CMORPH, PERSIANN and GPCP)	13 years (2002–2015)	CHIRPS and TRMM have a good agreement with in-situ at all spatiotemporal scales. All products were poorly performed for topography (m.a.s.l.) > 2500. Both CMORPH and TRMM overestimated on a daily scale.	(Gebremicael et al., 2017)

the performance of rainfall products at diverse elevations, and 12 river basins in Ethiopia. Temporal validation includes daily, monthly, and annual scale validation on a national scale. Furthermore, the seasonal scale validation was considered to understand the capability of rainfall products in recurrent drought-affected. This study aims to identify the best-performing products to support decisions in water resource management, drought and flood risk management, and climate studies in Ethiopia. Furthermore, the outcome will benefit neighboring countries of Ethiopia that are heavily dependent on streams originating from the highlands of Ethiopia.

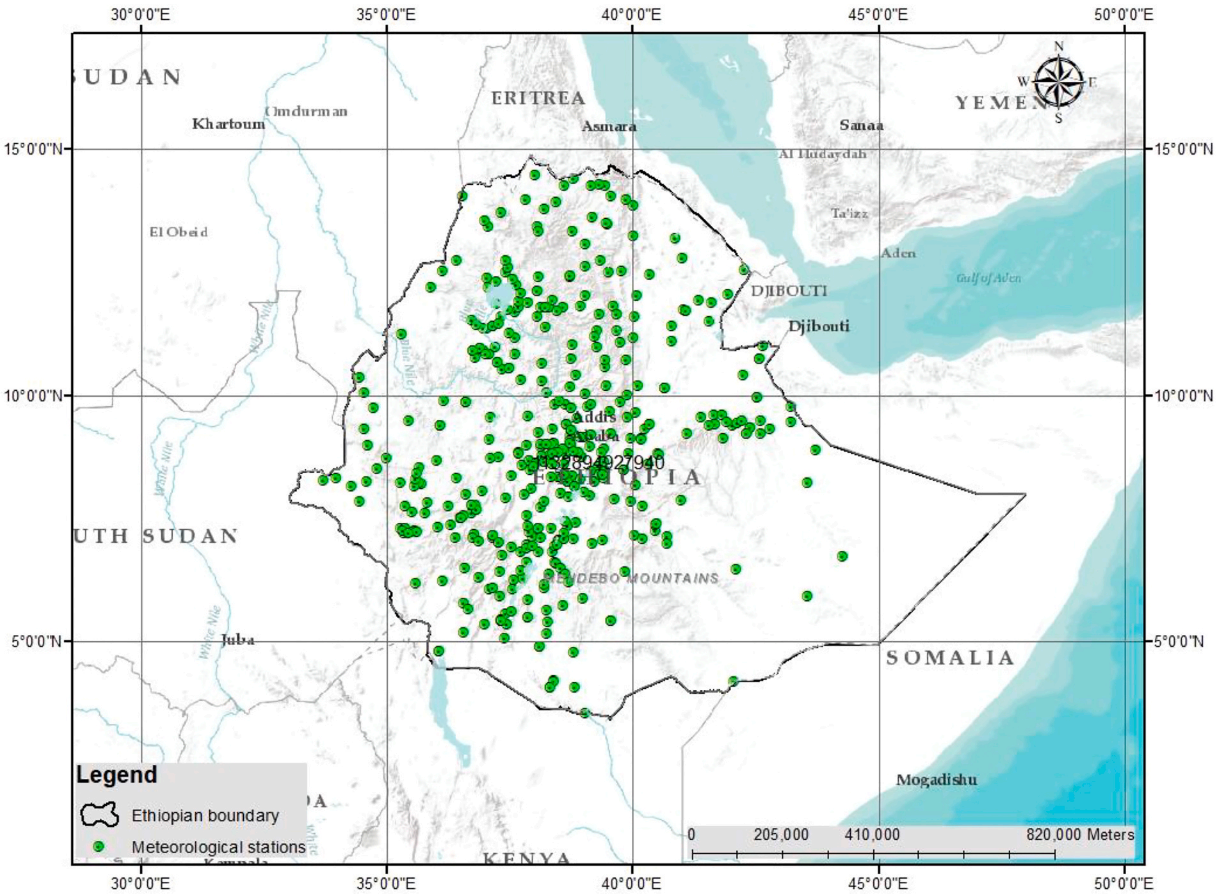

Fig. 1. Map of the study area, where the red dots represent the conventional gauge meteorological stations considered in the study.

2. Data and methodology

2.1. Description of the study area

Ethiopia is located in the Horn of Africa, which is a region in Eastern Africa (Fig. 1) and is known for its diverse climate, which includes tropical to temperate characteristics (Korecha and Barnston, 2007). The diverse hydrophysical and landscape features make this country unique in the region. Multiple weather systems, particularly large climate signals, determine the seasonality and distribution of rainfall in Ethiopia (NMA, 1996). The mean annual distribution of rainfall extends from approximately 200 mm over the north eastern and south eastern parts of the country to more than 1800 mm in the highlands of Southwest Ethiopia (Cheung et al., 2008).

This study focused on the validation of satellite-based and reanalysis rainfall estimate products for Ethiopia via multiple climate classification approaches (Fig. 2A, Fig. 2B, and Fig. 2C), topography, river basins, and recurrent drought-affected regions.

The elevation of the country (Fig. 2D) ranges from 125 m below sea level in the northeast to more than 4620 m above sea level in the central north (Abate et al., 2020), and the country is divided into 12 major river basins (Fig. 2 E). The eastern and southeastern parts of the country experience recurrent droughts that lead to major environmental and social challenges, which affect the livelihoods of pastoral and agro-pastoral communities in the region (Fig. 2 F). In total, 430 conventional ground weather station (hereafter, in-situ or gauge) data measured across the country were considered in this study.

2.2. Dataset

2.2.1. Satellite-based rainfall estimate (SbRE) dataset

This section describes the SbRE and reanalysis datasets used for validation. In this study, ten gridded open-source rainfall products

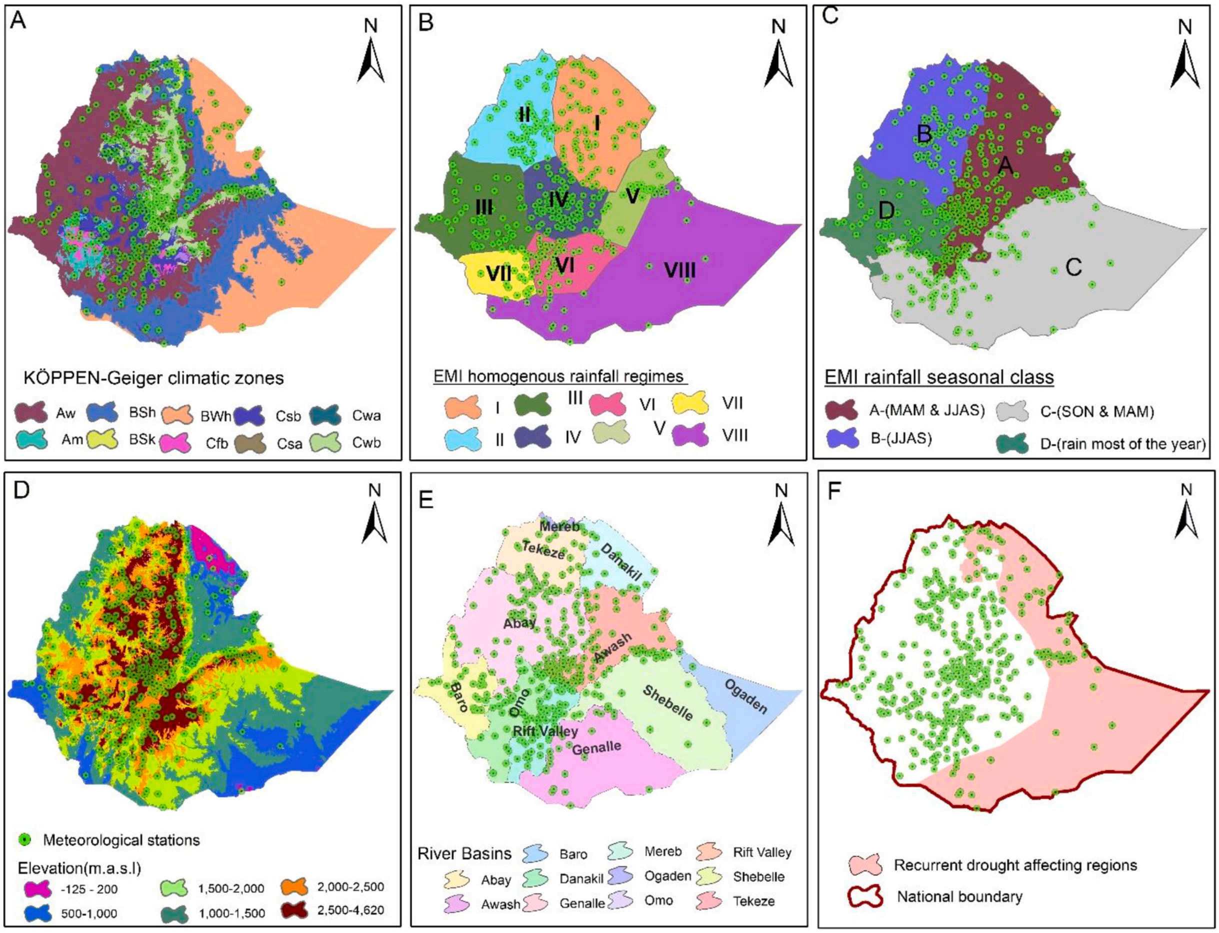

Fig. 2. Hydrophysical and landscape classification of Ethiopia, and relative meteorological station distributions are indicated on the maps of: the Köppen-Geiger Climatic Zone (A), Homogenous Rainfall Regions (B), Seasonal Rainfall Regions (C), Topography (D), River Basins (E) and Recurrent drought affected regions (F).

were considered for validation from 2001 to 2020, except the SM2RAIN rainfall product that was available starting 2007. Among the ten products, nine were satellite-based rainfall estimates (SbRE), and one was a reanalysis rainfall product. Among the nine SbRE products, eight were gauge-corrected satellite rainfall estimates, and one was a soil moisture retrieval-based rainfall estimate (SM2RAIN). The products were chosen for the following three reasons:

a) The SbRE products performed well in repeated evaluations across different catchments or basins in Ethiopia. For example, the performance of IMERG in different catchments across Ethiopia was found to be reasonably good for various purposes (Adane, Hirpa, Lim, et al., 2021; Kawo et al., 2021; Mekonnen et al., 2022). In this specific study, a national scale evaluation helped identify comparative performance at the country scale for products that had been identified as having good performance in a part of the country and validated their representativeness at a wider national scale.
b) Rainfall estimates products that have contradictory outcomes in different studies for the same SbRE product and in the same study area: SbRE products that were repeatedly used for evaluation in different parts of Ethiopia and their evaluation outcome represented by mixed results for the same location. For example, CMORPH was selected because (Bitew and Gebremichael, 2011) has documented that this product is more consistent and reliable; however, (Cha et al., 2014) categorized it as a product that suffers

Table 2
Description and summary of the SbRE and reanalysis rainfall estimate products considered in this study.

Dataset and product version	Name	Spatial resolution (°)	Spatial coverage	Temporal resolution	Latency	Reference	Source and download link
CMORHP v2.0	Climate Prediction Center's morphing technique	0.25	global	Daily	~1day	(Joyce et al., 2004)	NOAA Climate Data Record (CDR) https://www.ncei.noaa.gov/products/climate-data-records/precipitation-cmorph
IMERG-F v6B	Integrated Multisatellite Retrievals for Global Precipitation Measurements	0.1	Global	Daily	~2.5 months	(Huffman, G.J. et al. (2020)	NASA GESDISC DATA ARCHIVE: https://gpm1.gesdisc.eosdis.nasa.gov/data/GPM_L3/GPM_3IMERGDF.06/
RFEv2.0	Rain Fall Estimates	0.1	Africa	Daily	~2 days	(Love et al., 2004)	USGS FEWS NET: https://edcintl.cr.usgs.gov/downloads/sciweb1/shared/fews/web/africa/daily/rfe/downloads/daily/
ARC v2.0	Africa Rainfall Climatology	0.1	Africa	Daily	2 days	(Gebrechorkos et al., 2018)	NOAA / NWS / NCEP/ Climate Prediction Center:https://ftp.cpc.ncep.noaa.gov/fews/fewsdata/africa/arc2/geotiff/
CHIRPSv2.0	Climate Hazards Group InfraRed Precipitation with Station Data	0.05	50°	Daily	~3 weeks	(C. C. Funk et al., 2014)	Climate Hazard Center (CHC): https://data.chc.ucsb.edu/products/CHIRPS−2.0/africa_daily/tifs/p05/
PERSIAN-CDR	Precipitation Estimation from Remotely Sensed Information Using Artificial Neural Networks Climate Data Record	0.25	60°	Daily	~6 months	(Nguyen et al., 2018)	Centre for Hydrometeorology and Remote Sensing (CHRS) at the University of California https://chrsdata.eng.uci.edu/
SM2RAIN-ASCAT	Satellite rainfall data from ASCAT soil moisture observations	0.1	Global	Daily	~ 1 day	(Brocca et al., 2019)	National Research Council of Italy: http://hydrology.irpi.cnr.it/download-area/sm2rain-data-sets/
TAMSATv3.1	Tropical Application of Meteorology Using Satellite Data and Ground-Based Observations	0.0375	Africa	Daily	~2 days	(Maidment et al., 2017)	University of Reading: https://gws-access.jasmin.ac.uk/public/tamsat/rfe/data_zipped/v3.1/daily/
MSWEP v2.8	Multi-Source Weighted-Ensemble Precipitation	0.1	Global	daily	Few months	(Shaowei et al., 2022)	GloH20:https://drive.google.com/drive/folders/1Kok05OPVESTpyyan7NafR−2WwuSJ4TO9
ERA5	ECMWF Reanalysis	0.25	Global	Hourly	~ 5 day	(Hersbach et al., 2020)	European Centre for Medium-Range Weather Forecasts https://cds.climate.copernicus.eu/cdsapp#!/software/app-c3s-daily-era5-statistics?tab=app

from poor performance and high positive bias in the same upper Blue Nile subbasins. This comprehensive validation was expected to provide the best performance category via multiscale assessment and to show the comparative performance of multiple products.

c) The purpose of the designed products is related to Ethiopian natural phenomena and data availability. For example, Ethiopia is commonly affected by recurrent droughts (WBG, 2020), and CHIRPS is commonly used by drought monitoring institutions (for example: FEWSNET, https://fews.net) as it was created for early warning of drought (C. Funk et al., 2015). TAMSAT was generated to study African rainfall (Maidment et al., 2014), and SM2RAIN-ASCAT was designed to fill the space and time inconsistency gap of rainfall data by conducting a "bottom-up" observation approach by utilizing satellite soil moisture observations (Brocca et al., 2019).

Table 2 provides a summary of the selected SbRE product, data version, spatial and temporal resolutions, spatial coverage, latency, and source of the data. Briefly describe the major algorithmic features or development background of SbRE products:-

CMORHP v2.0 (hereafter referred to as CMORHP) was developed by the National Oceanic and Atmospheric Administration (NOAA) Climate Prediction Center and uses geostationary infrared (IR) and low-orbit passive microwave (PMW) data to estimate precipitation; it uses mainly PMW data, whereas IR is considered for interpolation in the absence of PMW data.

IMERG-F v6B (hereafter referred to as IMERG) is the successor of the Tropical Rainfall Measuring Mission (TRMM) product, and its algorithm uses gauge data to correct the bias of the product estimated by combining IR data from geostationary satellite observations and PMW data from global rainfall measurement constellation satellites.

RFEv2.0 (hereafter referred to as RFE) is the data produced by the National Oceanic and Atmospheric Administration (NOAA) Climate Prediction Center (CPC) for the Famine Early Warning Systems Network to assist in disaster monitoring activities over Africa; its algorithm incorporates gauge PMW and infrared data from METEOSAT geostationary satellites.

ARC v2.0 (hereafter referred to as ARC) focused only on Africa and was designed by NOAA-CPC. Its algorithm combines inputs from two primary sources: 3-hourly geostationary IR data cantered over Africa provided by EUMETSAT and quality controlled by Global Telecommunication System (GTS) gauge observation.

CHIRPSv2.0 (after this CHIRPS) was developed by the US Geological Survey (USGS) and the Climate Hazards Center of the University of California Santa Barbara; its algorithm combines ground observations, thermal IR data from quasiglobal geostationary satellite observations, MW data from the TRMM, and precipitation climatology data.

PERSIAN-CDR was developed by the University of California, Center for Hydrometeorology and Remote Sensing (CHRS), and uses an artificial neural network (ANN) to merge IR, PMW, and gauge data. It uses GPCP monthly rainfall data for bias adjustment.

TAMSATv3.1 (hereafter referred to as TAMSAT), the necessity to monitor rainfall deficits and their impact on crop yield across the Sahel and southern Africa regions, is the motivational factor for TAMSAT generation; its algorithm uses thermal infrared (TIR) imagery from the Meteosat satellites of EUMETSAT and calibrates the Cold Cloud duration (CCD) via gauge observations.

MSWEP v2.8 (hereafter referred to as MSWEP) algorithm merges a large number of input data, such as: gauge data, satellite-based precipitation estimates (e.g GSMaP and CMORPH), and reanalysis data (e.g ERA5 and JRA-55). It is unique for correcting the gauge reporting time for incorporated daily gauges to enhance the performance.

The ERA5 reanalysis product of the ECMWF and algorithm combine an enormous number of historical observations through modelling and data assimilation systems. It incorporates both liquid and frozen precipitation falling on the earth.

SM2RAIN-ASCAT, unlike all other SbRE products, uses the "bottom-up" approach estimation of satellite rainfall, where it uses the SM2RAIN algorithm to convert satellite soil moisture data into rainfall estimates via the SM2RAIN algorithm (soil moisture to rain).

2.2.2. In-situ dataset

Daily time series of in-situ rainfall data were collected from the Ethiopian Meteorological Institute (EMI) from 2001 to 2020, among the longest daily time series data considered for validating SbRE in Ethiopia (see Table 1). In-situ data were selected on the basis of their spatial representation, availability of continuous records, and consistency. As part of the data quality check procedure, a double mass curve (Searcy and Hardison, 1960) was used to filter out inconsistent time series in-situ data. Initially, data from 467 stations were selected for screening; however, only 430 stations were selected using a double mass curve for the evaluation of SbRE. In this one-to-one evaluation approach, missing in-situ data were not imputed; instead, the corresponding SbRE data were excluded. Additionally, in-situ data with more than 37 % missing values were deemed inconsistent and therefore not included in the analysis. Fig. 2 shows the spatial representation of the number of meteorological stations and the percentage of missed in-situ data in different climate, river basin, and topography classification categories.

2.2.3. Climate classification dataset

Studies have shown that SbRE and reanalysis rainfall product performance can be affected by climate (Mekonnen et al., 2023; Ogbu et al., 2020; Zambrano-bigiarini et al., 2017). In this study, in addition to climate, the effect of climate categorization on performance evaluation was also addressed, which was overlooked by previous studies. Rainfall products were validated in three different climate classification types considered in this study: the Koppen-Geiger climatic zone classification, homogenous rainfall regions currently used by EMI, and rainfall regimes classified by the EMI on the basis of seasonal rainfall patterns.

2.2.4. Köppen-Geiger climatic zone classification

The Köppen-Geiger climate zone classifies the global climate into five main and 30 subclasses on the basis of threshold values and seasonality of monthly precipitation and temperature(Beck et al., 2018; Kottek et al., 2006). According to this approach, Ethiopia is represented by ten climate classes, namely, Tropical Savanna, dry winter (Aw), Tropical Monsoon (Am), Dry Semi-Arid hot (BSh), Dry

Semi-Arid cold (BSk), dry arid desert hot (BWh), Temperate no dry weather hot summer (Cfb), temperate dry and warm summer (Csb), temperate dry winter and hot summer (Cwa), and temperate dry winter and warm summer (Cwb). In this study, the distribution of in-situ data in each Köppen-Geiger climate zone is presented in Fig. 2A. Two categories of the Köppen-Geiger climate zone, classes Csa and Cwa, were omitted in this study since each class was represented by only one in-situ dataset, which is too few in number to represent the spatial scale of each climate category.

2.2.5. EMI homogenous rainfall regions

Fig. 2. B describes the homogenous rainfall region used by the Ethiopia Meteorological Institute for the seasonal rainfall prediction preparation. Accordingly, the homogenous rainfall region of Ethiopia is classified into eight regions: Region I = northeast, Region II = northwest, Region III = southwest, Region IV = central, Region V = east, Region VI = south highland, Region VII =south, and Region VIII = south—southeast lowlands(Korecha and Sorteberg, 2013).

2.2.6. EMI seasonal rainfall regime classification

Ethiopian seasonal rainfall climatology is predominantly determined by a large amount of climate circulation, particularly the movement of the intertropical convergence zone (ITCZ) (Nicholson, 2017) and complex topography across the country (Korecha and Barnston, 2007). On the basis of seasonal rainfall patterns, the Ethiopian Meteorological Institute (NMA, 1996) categorized the country into four rainfall regimes (Fig. 2C) for seasonal weather forecast application, namely: Region A, which receives the highest rainfall from June to September (locally named Kiremet) and the second highest from March to May (locally named Belg); Region B, which includes June to September (Kiremet); Region C, which includes March to May (Belg) and September to November; and Region D, which contains every rainy region with peak amounts between July to September.

2.2.7. Supplementary spatial datasets

Additional spatial datasets used in this study include topography (Fig. 2D), generated via a 30 × 30 m digital elevation model (DEM) from Shuttle Radar Topography Mission (SRTM) Global (NASA Shuttle Radar Topography Mission (SRTM), 2013). The shape files for 12 river basins in Ethiopia (Fig. 2E) were collected from the Ministry of Water and Energy of Ethiopia. The sub-basin data was extracted from HydroSHEDS (https://www.hydrosheds.org/products/hydrobasins) to present the four most representative SbRE products tailored from the analysis for applications in flood risk management and water resource management. This selection aims to available SbRE as a complementary source of information in gauge data for decision support. Additionally, the analysis incorporated the latest regional and zonal administrative boundary data for Ethiopia, which was sourced from the United Nations Office for the Coordination of Humanitarian Affairs (OCHA) of Ethiopia. Administrative spatial data integration supports the identification of suitable four SbRE products for climatological studies and drought monitoring applications. The recurrent drought-affected arid and semi-arid regions of Ethiopia (Fig. 2F) were filtered on the basis of historical drought event studies and humanitarian response reports (Fich, 2022; Korecha and Barnston, 2007; Mera, 2018).

2.3. Methodology

2.3.1. Data extraction, spatial and temporal evaluation representation

As the gauge station (in-situ) distribution is uneven and sparsely disseminated in substantial areas of the country, particularly in the entire border area, a pixel-to-point comparison was applied between SbRE and the reanalysis products against the ground observation dataset. The chosen SbRE grid data have different resolutions (e.g. CMORP=0.25 degree to TAMSAT 0.0375 degree) (see Table-2); however, extraction of data from the pixel-based SbRE uses the original resolution to avoid the uncertainty that may be introduced by resampling, and any point in the pixel is summed to be representative of the ground observation regardless of the point of extraction within the pixel(Garba et al., 2023; Qureshi et al., 2022).

A multiscale evaluation of ten gridded rainfall products was conducted against 430 in-situ meteorological station-based observations. The evaluation was conducted at different spatial scales: the national scale, three different climate classification approaches that include eight climatic zones according to the Koppen-Geiger classification (Fig. 2-A), eight EMI classifications based on homogenous regions (Fig. 2-B), and four EMI seasonal rainfall regimes (Fig. 2-C). Furthermore, seven elevation classes (Fig. 2-D), 12 river basin scales (Fig. 2-E), and recurrent drought-affected regions (Fig. 2-F) were used. Through the Ethiopian topography, the range extends from 125 m below mean sea level to 4620 m above mean sea level, and only stations at an elevation starting at zero mean sea level were considered. Accordingly, the country was divided into seven elevation classes: 0–200 m, 200–500 m, 500–1000 m, 1000–1500 m, 1500–2000 m, 2000–2500 m, and > =2500 m. Each spatial classification category, the number of ground observations (in-situ data), and the percentage of missed data of each class are presented in Fig. 2 A - Fig. 2-F.

The temporal scales were considered daily, monthly, seasonal, and annual at the national spatial scale. The daily data were summed to generate all other temporal scale data for both the SbRE and the in-situ data. Four seasonal wet-season rainfall categories (MAM and JJAS of regime-A, and MAM and SON of regime-c) (see Fig. 2C) were considered in the arid and semi-arid recurrent drought-affecting regions of Ethiopia.

The four seasonal rainfall periods vary in location, as explained in Section 2.2.3 C. To further validate the ability of the rainfall products to capture drought, validation was conducted on a monthly basis, only for drought years, and only for drought years during the wet season's months of recurrent drought-affected parts of the country (Fig. 2-F).

2.3.2. Performance evaluation approach

Two groups of statistical analyses were performed to validate the SbRE and reanalysis products. Accordingly, five pairwise or continuous and six categorical statistical evaluations were performed at different spatial scales. As summarized in Table 3, among the chosen statistical metrics of continuous performance, linear correlation (R) was used to determine how good rainfall products are in comparison with in-situ bias metrics, indicating how the mean value of SbRE captures the corresponding mean value of ground observations. The coefficient of variation (CV) was used to compare the dispersion between the SbRE products and in-situ values. Kling Gupta efficiency (KGE) decomposes the total performance of SbRE and reanalysis products into linear correlation (R), bias ratio (bias), and coefficient of variation (CV) values. KGE is an important index that represents the temporal dynamics, volumetric capturing ability, and variability of rainfall at the same time. Bias is used to understand the overestimation or underestimation of SbRE compared with in-situ data.

Categorical performance metrics were used to evaluate the SbRE and reanalysis product detection abilities for different rainfall intensities across Ethiopia by modifying the rainfall intensity categories classified by both the Ethiopian Meteorological Institute (NMA, 2015)and the WMO classification (W. Wang et al., 2021). Accordingly, in this study, satellite-based rain intensity was classified as no rain (< 1 mm/day), very light rain (between 1 mm/day and 5 mm/day), light rain (between 5 mm/day and 10 mm/day), moderate rain (between 10 mm/day and 30 mm/day), or heavy rain (> 30 mm/day).

Table 4 summarizes the contingency table of the categorical metrics used in the detection of SbRE (Toté et al., 2015). To compare gauge and satellite data in the context of rainfall measurement, indicated as Hit (A) when both the satellite and gauge measurements indicate rainfall, False Alarm (B) instances where the satellite indicates rainfall, but the gauge does not, Miss (C) when the gauge indicates rainfall, but the satellite does not, and Correct Negative (D) when both the satellite and gauge measurements indicate no rainfall. The false alarm ratio (FAR) and probability of detection (POD) indicate that a fraction of the estimated events did not occur and that a fraction of the observed events were correctly estimated. The frequency bias (FB) shows systematic differences between the occurrence of rain events in-situ observations and SbRE. The equitable threat score (ETS) indicates how correctly SbRE events agree with in-situ events and can be used to evaluate hits by chance. The critical success index (CSI) indicates the relative value of SbRE over in-situ observations. The Heidke skill score (HSS) reflects the accuracy of the SbRE estimates accounting for matches in-situ owing to random chance.

3. Results and discussion

3.1. Daily product validation

Fig. 3 shows a box plot summarizing the temporal scale comparative performances among the ten rainfall estimation products on a daily, monthly, and yearly basis. The median values for the KGE, R, and RMSE are presented in Table 5. Considering the median values of the performance indicators, the performance of all ten daily rainfall estimate products is poor; however, the CMORHP, MSWEP, IMERG, and CHIRPS products ranked relatively higher than the other datasets for daily rainfall estimation. The better comparative

Table 3
Continues and categorical performance metrics applied in this study.

Performance metric class	Statistical metric	symbol	Formula	Perfect match
Continuous	Bias ration	Bias	$\text{Bias} = \frac{\sum \text{SbRE}}{\sum \text{Insitu}}$	1
	Correlation	R	$\text{R} = \frac{\sum_{i=1}^{N}(\text{Insitu} - \overline{\text{SbRE}})(\text{Insitu} - \overline{\text{Insitu}})}{\sqrt{(\text{SbRE} - \text{SbRE})^2}(\sqrt{(\text{Insitu} - \overline{\text{Insitu}})^2}}$	1
	Coefficient of Variation	CV	$\text{CV} = \frac{CV_{SBRE}}{CV_{Insitu}}$	1
	Kling Gupta Efficiency	KGE	$\text{KGE} = 1 - \sqrt{(\text{R}-1)^2 + (\text{Bias}-1)^2 + (\text{CV}-1)^2}$	1
	Root Mean Square Error (mm)	RMSE	$\text{RMSE} = \frac{\sqrt{\sum_{i=1}^{N}(\text{SbRE} - \text{Insitu})^2}}{\sum_{i=1}^{N}\text{Insitu}}$	0
Categorical	Probability Of Detection	POD	$\text{POD} = \frac{\text{A}}{\text{A}+\text{C}}$	1
	False Alarm Ratio	FAR	$\text{FAR} = \frac{\text{B}}{\text{A}+\text{B}}$	0
	Frequency of Bias Index	FBI	$\text{FBI} = \frac{\text{A}+\text{B}}{\text{A}+\text{C}}$	1
	Equitable threat score	ETS	$\text{ETS} = \frac{(\text{A} - A_r)}{(\text{A}+\text{B}+\text{C}-A_r)}$ with hits that occur by chance:$A_r = \frac{((A+C)(A+B))}{A+B+C+D}$	1
	Critical Success Index	CSI	$\text{CSI} = \frac{\text{A}}{(\text{A}+\text{C}+\text{B})}$	1
	Heike skill score	HSS	$\text{HSS} = \frac{(2(AD-BC))}{((A+c)(C+D)+(A+B)(B+D))}$	1

Table 4
Contingency table used for analysing the detection ability of the rainfall products.

SbRE and reanalysis estimates	Gauge (in situ) measurement		
	Yes	No	Total
Yes	Hit(A)	False Alarm(B)	A+B
No	Miss(C)	Correct Negative (D)	C+D
Total	A+C	B+D	A+B+C+D

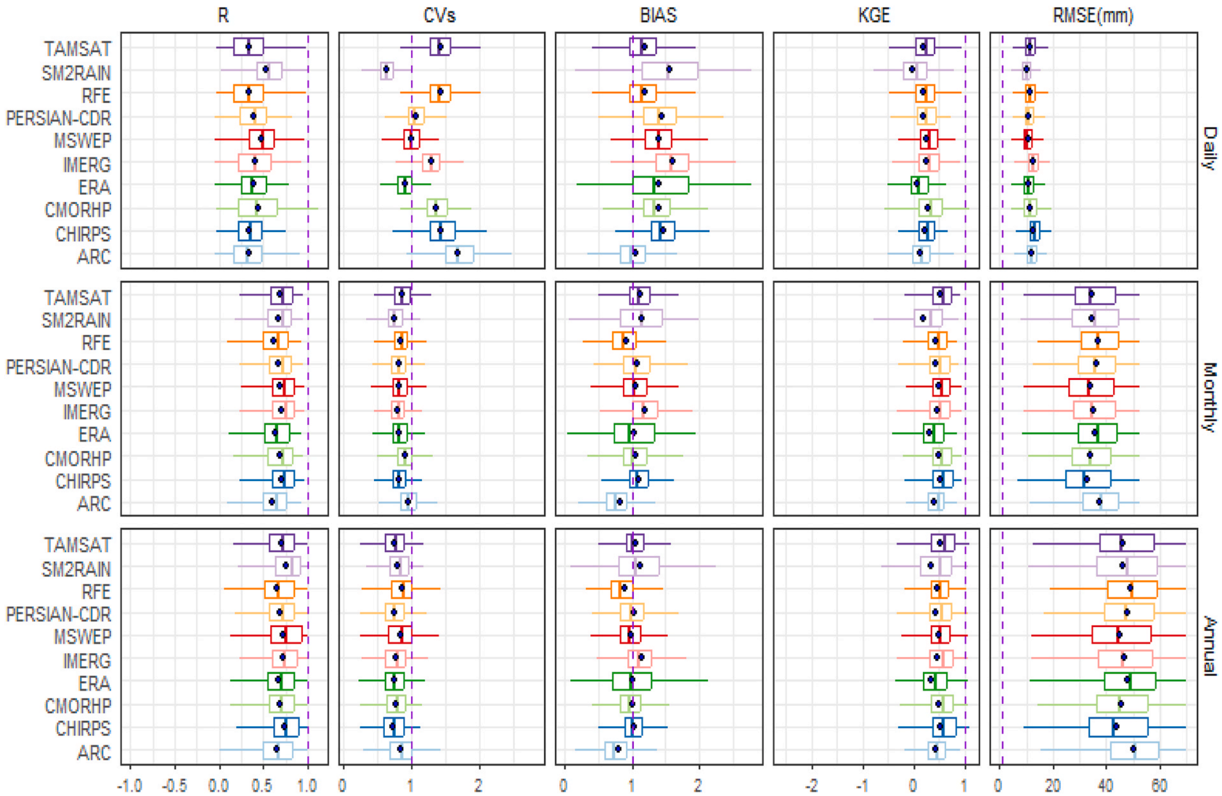

Fig. 3. Five continuous metrics results show a comparative representation of ten SbRE and product performance over Ethiopia at three different timescales. The purple dashed line represents the optimal value of each metric. The left and right ends of the boxes in the boxplot represent the 25th and 75th percentiles of each product's performance, respectively, whereas the bold solid line in the middle of the boxes represents the median value, and the dark blue dots represent the mean value.

Table 5
Median values of ten SbRE and reanalysis of rainfall products on the basis of the continuous evaluation metrics.

Rainfall products	Daily			Monthly			Annual		
	KGE	R	RMSE	KGE	R	RMSE	KGE	R	RMSE
ARC	0.11	0.22	8.17	0.48	0.65	73.71	0.46	0.67	50.69
CHIRPS	0.19	0.24	8.92	0.66	0.75	65.68	0.67	0.76	42.58
PERSIAN-CDR	0.18	0.28	7.5	0.53	0.72	69.30	0.54	0.72	47.30
TAMSAT	0.16	0.24	7.95	0.58	0.72	67.44	0.57	0.73	45.46
CMORHP	0.24	0.3	7.49	0.65	0.73	67.77	0.67	0.70	44.95
IMERG	0.21	0.29	8.51	0.53	0.75	67.71	0.56	0.74	46.21
MSWEP	0.22	0.32	7.22	0.67	0.75	65.66	0.68	0.76	44.25
RFE	0.16	0.24	7.95	0.50	0.67	72.32	0.53	0.67	49.44
ERA5	0.07	0.26	7.63	0.40	0.66	78.86	0.42	0.71	48.90
SM2RAIN	0.05	0.39	6.94	0.41	0.73	82.04	0.53	0.82	47.96

performance of these four rainfall products relative to the other products may be associated with the better utilization of gauge data and their merging approaches for improving the products. Fig. 3 further shows that the KGE values of the CMORPH, MSWEP, IMERG, and CHIRPS products range from −1.58–0.75, from −1.27–0.58, from −1.7–0.63 and from −1.16–0.47, respectively. Similarly, the RMSE values increased from 3.0 mm to 13.7 mm, from 2.23 mm to 14.9 mm, from 3.67 mm to 14.69 mm, and from 2.0 mm to 14.6 mm, respectively, for each product. We also found that the KGE tended to be closer to the optimal value (KGE=1), improved monthly and annually, and had a large value of RMSE (mm) in both the monthly and annual time steps.

In general, all ten rainfall products overestimate the daily amount and are poor in terms of continuous evaluation metrics. A possible reason for the poor performance of daily rainfall estimates could be associated with the algorithms used for rainfall or the type of satellite sensors (Ayat et al., 2021; Toté et al., 2015), atmospheric interference or cloud coverage impact (Satgé et al., 2019; Tapiador et al., 2018), calibration issues (Mekonnen et al., 2021; Kuligowski, 2002; Kuligowski et al., 2016; TAMSAT Group, 2016), high spatial variance, and absence of a dynamic range for daily rainfall estimates (Mekonnen et al., 2023).

Fig. 4 represents the accuracy of the rainfall estimation products in detecting daily rainfall across Ethiopia. All the rainfall products performed better at detecting "no rain" or rainfall less than 1 mm with the lowest POD value of 0.7 (PERSIAN-CDR) and the highest value of 0.87 (CHIRPS). Considering the POD value, comparable results were obtained for ARC, CHIRPS, CMORHP, TAMSAT, and SM2RAIN, in order of performance, for detecting rainfall less than 1 mm. Very light rain (between 1 mm/day and 5 mm/day) was relatively better captured by MSWEP, RFE, and PERSIAN-CDR, with ETSs ranging between 0.17 and 0.19 and PODs ranging between 0.34 and 0.37.

All product detection skills were poor for moderate (between 10 mm/day and 30 mm/day) and heavy (> 30 mm/day) rainfall. These findings are in line with several other studies(Nashwan et al., 2020; Rahmawati and Lubczynski, 2018; Zambrano-bigiarini et al., 2017) that revealed similar findings regarding the poor performance of the same rainfall estimation products in detecting high-intensity rainfall. The possible cause for the poor performance of the rainfall products at high rates is limited temporal coverage, which results in the absence of short-duration rain (Burdanowitz et al., 2015), limitations in retrieval algorithms (Kidd et al., 2003), technical limitations, such as beam blockage in complex trains (McRoberts and Nielsen-Gammon, 2017; Vivekanandan et al., 1999), and vertical profiling techniques that commonly struggle to capture high rainfall rates (Thakur et al., 2019). However, IMERG, RFE, and CMORPH exhibited relatively better detection abilities for heavy rainfall than the other products did. Some studies have identified the same rainfall products with better detection abilities for high-rate rainfall, such as IMERG in East Africa (Mekonnen et al., 2023), CHIRPS (Bai et al., 2018), and CMORPH (G. Wang et al., 2017).

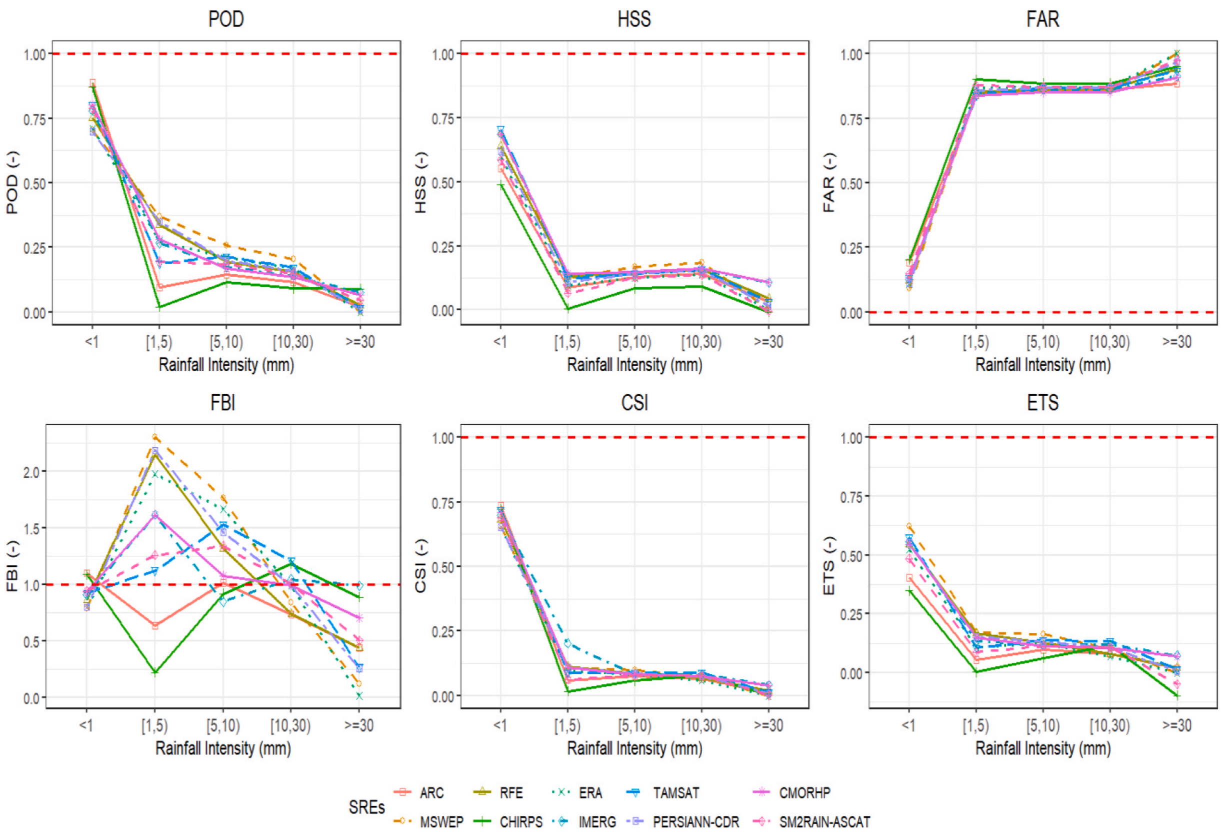

Fig. 4. Daily rainfall detection ability of SbRE and reanalysis of rainfall product (median) values via six categorical metrics. A red dashed line represents the optimal value of each categorical performance metric.

Under normal circumstances, when POD and ETS are high, the FAR is expected to be low(Toté et al., 2015). As indicated in Fig. 4, the rainfall in some parts of the country that are commonly known to receive moderate-to-high rainfall intensities (rainfall greater than 10 mm) was underestimated by SbRE. This could occur when the rainfall intensity is greater than 10 mm, it surpasses temporal sampling; coarse spatial resolution(He et al., 2023; Park et al., 2017), and cloud attenuation (Kumar, 2021; Battaglia et al., 2020) could be other reasons for the underestimation.

Both the ARC and CHIRPS behave differently for rainfall in the 1 mm–5 mm range (FBI <1) than the other products do. The main reason for this could be related to the algorithms used to develop each product. The bias of rainfall < 1 mm could vary by underestimation or overestimation relative to the gauge data, depending on the climatic situation of each area. Satellite rainfall estimates that the products overestimate very light rainfall (Fig. 4, FBI rain rate < 5 mm/day) in arid or semiarid regions owing to subcloud evaporation, in which rain evaporates before it reaches the ground (Sarkar et al., 2023). Importantly, the bias in very light rainfall could also lead to incorrect decisions in drought analysis and low-flow analysis of rivers.

The daily categorical metric-based statistical evaluation results of these rainfall products will guide users in selecting the best-performing products for various applications, particularly for drought monitoring and flood risk analysis. The validation of ten satellite products provides a detailed picture of each product at the national scale. For example, some products may perform better in detecting light rainfall events (for example, ARC, CHIRPS, and TAMSAT), which has direct implications for drought analysis, whereas others may be more suitable for flood modelling (Toté et al., 2015). By analysing the statistical evaluation results, users can make informed decisions about which rainfall products to use for their specific needs.

3.2. Monthly and annual rainfall validation

Considering the median values of the KGE performance metrics (Fig. 3 and Table 5), the CHIRPS, MSWEP, TAMSAT, CMORHP, and IMERG rainfall estimate products, in order of performance, attained the optimal values better than those of all the other products at both the monthly and annual scales. At the monthly time scale, the highest median value was recorded for the CHIRPS, with a value of 0.66, and the lowest median value of the RMSE was 65.68 mm. In contrast, ERA5 (KGE=0.40, RMSE=78.86 mm) and SM2RAIN (KGE=0.41, RMSE=82.04 mm) had the lowest KGE and the highest RMSE.

Among all rainfall products, TAMSAT has the highest spatial resolution, and its performance aligns with that of several previous studies in Ethiopia (see Table 1). A study conducted at the continent Africa scale categorized TAMSAT as a poorly performed product

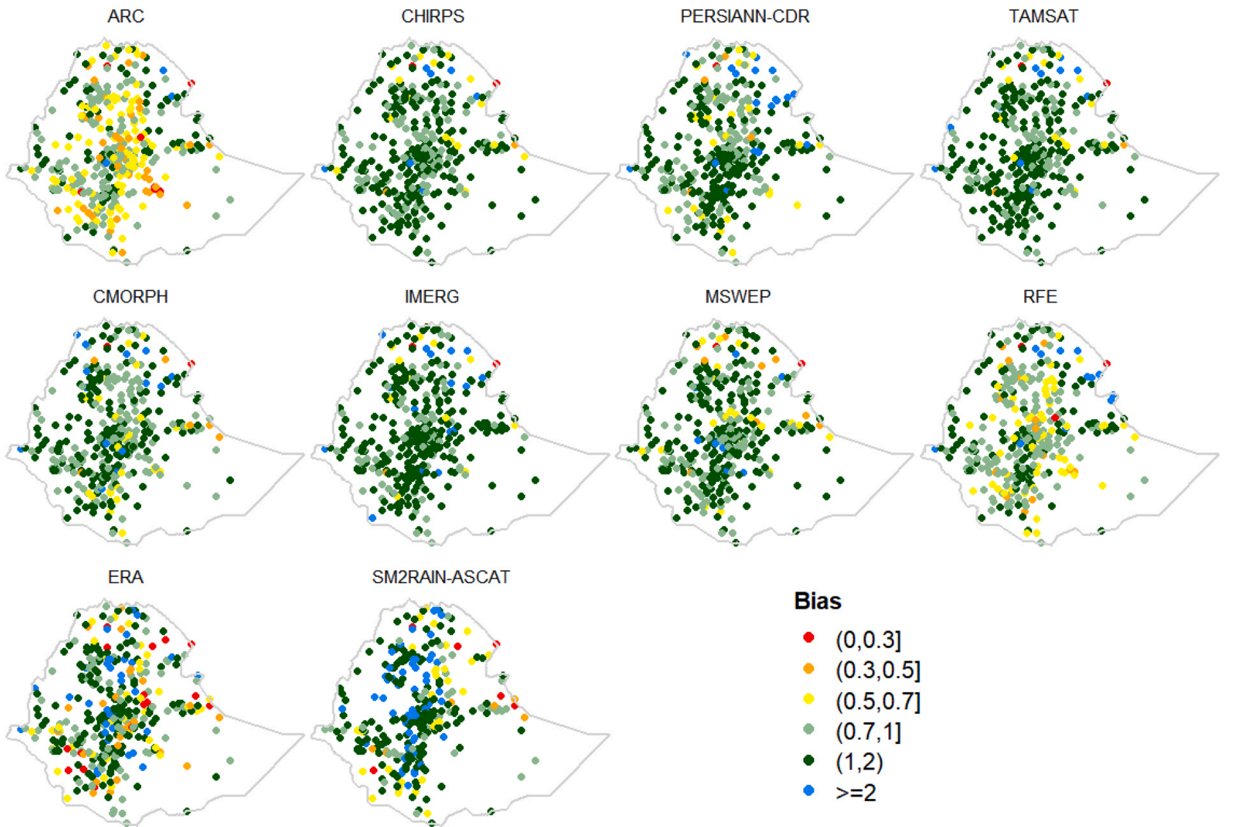

Fig. 5. Spatial representation of comparison between monthly gauge data and the corresponding satellite based and reanalysis rainfall products using bias performance metrics.

(Mekonnen et al., 2023), which shows that performance evaluation outcomes are highly affected by evaluation scales, such as continental, country, or small boundaries, due to the number of in-situ data from diverse climates. Furthermore, this implies that finer-resolution SbRE data do not always produce the best validation result compared with coarser-resolution data.

The median value of the bias performance metric marginally reached the optimal value (bias=1) for the CHIRPS, MSWEP, and CMOEPH rainfall products, in order of performance. In contrast, the SM2RAIN, PERSIAN-CDR, and IMERG rainfall products were overestimated, indicating poor performance (Fig. 2). The spatial representation of bias (Fig. 5) indicates the tendency of rainfall products to overestimate (Bias > 1), which indicated more green and blue colours and underestimate (Bias < 1) precipitation levels with extreme underestimation indicated by red colour revealed that ARC, ERA5, and RFE underestimated and SM2RAIN overestimated the monthly and annual observed values in the central highland area of the country. Hence, overestimating or underestimating products should be subjected to bias correction (Goshime et al., 2019; Gumindoga et al., 2016; Katiraie-Boroujerdy et al., 2020; Lober et al., 2023; Siddig et al., 2022; Xiang Soo et al., 2020) before being used as decision-supporting information.

Fig. 6 shows the coefficient of variation (CV) of ten SbRE and reanalysis rainfall products. The rainfall estimate products ARC, CMORPH, TAMSAT, and RFE, in order of performance, captured better rainfall variability than the other products did. All the rainfall estimation products presented greater variations at the daily timescales than at the monthly and annual timescales (Fig. 3). Importantly, temporal aggregation of daily data to monthly and annual time scales swaps random errors and improves the representativeness of monthly and annual data (Aghakouchak et al., 2012; de de de Moraes Cordeiro and Blanco, 2021; Hossain and Huffman, 2008; Maggioni et al., 2021; Schutgens et al., 2017).

3.3. Validation in different climate zone classification categories

Fig. 7 shows the monthly time scale KGE of ten rainfall estimates over Ethiopia based on three climate classification approaches, namely, the Köppen-Geiger climatic zone, homogenous rainfall regions, and similar seasonal rainfall pattern regions. The results revealed that the accuracy and preference of the best SbRE products were affected by climate systems and climate classification approaches. Accordingly, the accuracy level was different across the three climate classification approaches; however, four rainfall estimation products, CHIRPS, CMORHP, MSWP, and TAMSAT, outperformed all the other products in the three climate classification approaches.

The result based on Köppen-Geiger climatic zone classification revealed CHIRPS, TAMSAT, and CMORPH outperformed in tropical climates (Am and Aw), and MSEP and TAMSAT in arid climates (BSh, BSk, BWh). In the temperate category (Cfb, Csb, and Cwb),

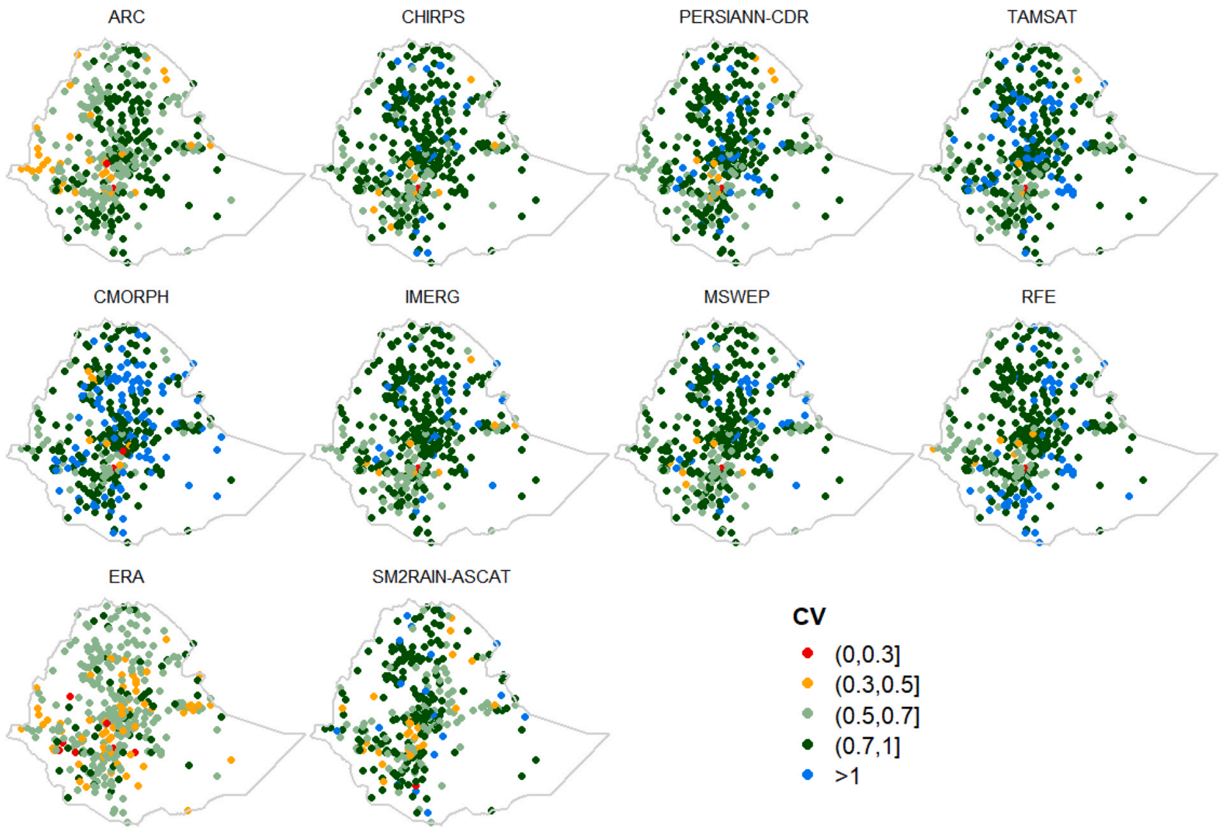

Fig. 6. Coefficient of variation of monthly satellite based and reanalysis rainfall estimate and the corresponding ground observation over Ethiopia.

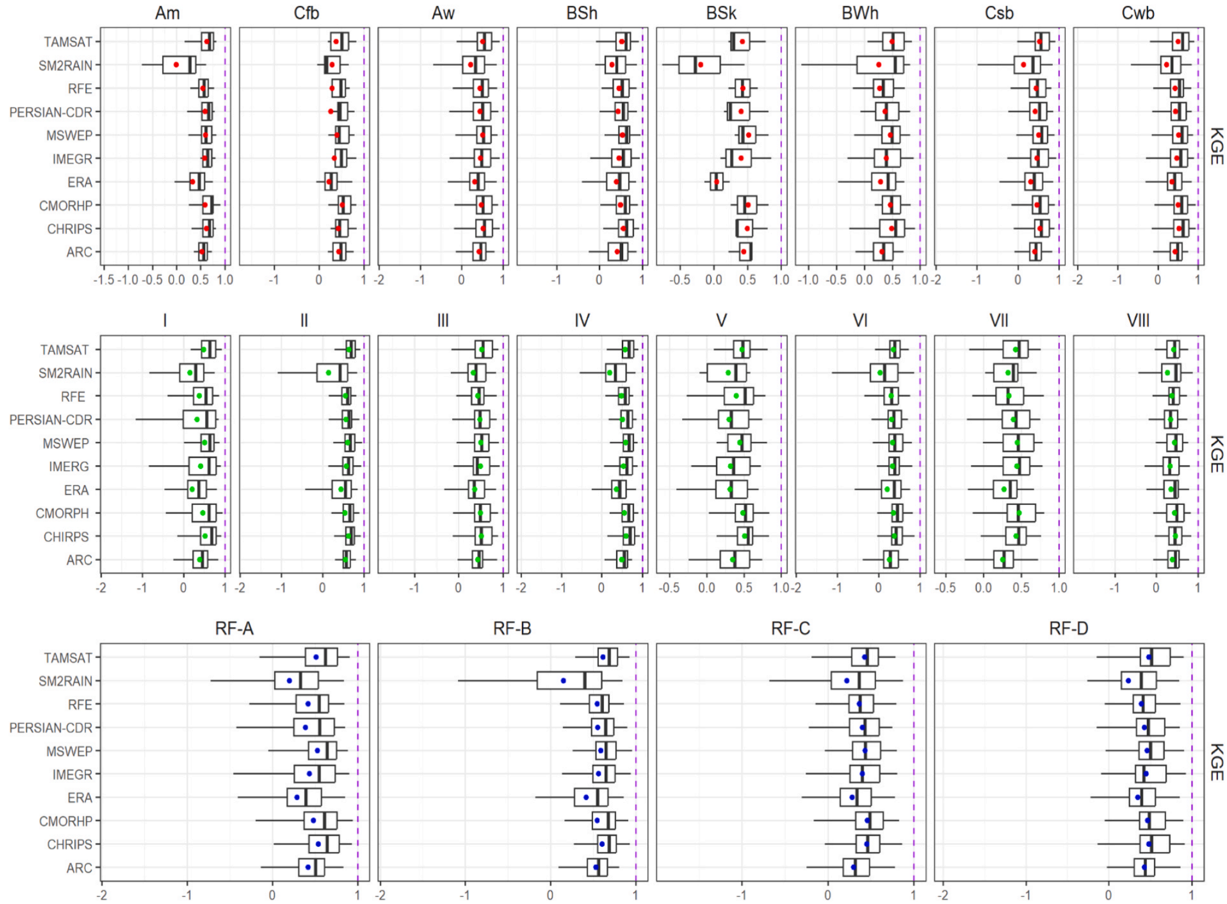

Fig. 7. KGE of ten SbRE and reanalysis rainfall estimates in three different types of climate classification approaches (top panel= Köppen-Geiger climatic zone classification, middle panel= homogenous rainfall regions, and bottom panel= EMI similar seasonal rainfall pattern regions) over Ethiopia. The purple dashed line indicates the optimal value of each performance metric. The right and left lines in the boxplot represent the 75th and 25th percentile, respectively. The vertical line in the box indicates the median value. The red, green, and blue dots represent the mean values of the performance metrics for the three types of climate classification.

CHIRPS and TAMSAT performed better than the other methods did. In contrast, both SM2RAIN and ERA consistently showed poor and high variation in the median value of KGE within the same climate class. However, SM2RAIN outperformed all products in the BWh climate class, where almost no gauge data were available and all eight gauges corrected SbRE inaccuracies, whereas SM2RAIN benefited from soil moisture data supported by the bottom-to-top observation approach algorithm. Overall, the satellite rainfall estimates performed better in tropical climates than in the arid and temperate classes of the Köppen-Geiger climatic zone classification, which is consistent with the findings of another study (Mekonnen et al., 2023), in addition to the difference in the choice of the best product in tropical and other climate classes. The performance difference in rainfall estimates in the Köppen-Geiger climatic zone classification could be associated with machine learning techniques used to blend satellite and reanalysis data to improve accuracy (Bhuiyan et al., 2019) and the representativeness of ground observation data used in each Köppen-Geiger climate class (Upadhyaya and Ramsankaran, 2016).

For validation in terms of homogenous rainfall regions (second panel of Fig. 7 and Table 6), in the majority of homogenous rainfall regions, CHIRPS, CMORPH, MSWEP, and TAMSAT were identified as the best-performing products. However, in three regions (IV, V, and V) where sharp spatial or elevation gradients were present, the KGE values for TAMSAT and IMERG were relatively lower than those of the other best-performing products. In contrast, the SM2Rain ERA and ARC perform poorly in the order of poor performance in regions with homogenous rainfall. A previous study indicated that the validation of SbRE based on homogenous rainfall regions often shows reasonable bias and accuracy, although it lags behind in-situ information in terms of precision(Massari et al., 2020). Compared with other climate classification approaches, the validation of SbRE in homogenous rainfall regions did not reveal fundamental changes in the preferences of rainfall products.

In similar seasonal rainfall pattern receiving areas (third panel of Fig. 7 and Table-6), CHIRPS and MSWEP presented the best performance, with a median KGE value of 0.64 for category A (RF-A), which receives the highest amount of rainfall during JJAS (Kirement) and the second highest amount of rainfall during MAM (Belg). In the rainfall regime of RF-B, the three rainfall products (CHIRPS, TAMSAT, and CMORPH) exhibited comparatively similar performances (KGE=0.69). In both the RF-C and RF-D regions,

Table 6
Median values of KGE for ten rainfall products (dark green represents KGE>0.6, light green represents KGE values between 0.5 and 0.59, light red represents values between 0.3 and 0.39, and dark red represents values less than 0.3).

Climate classification	Symbol	ARC	CHIRPS	PERSIAN-CDR	TAMSAT	CMORHP	IMEGR	MSWEP	RFE	ERA	SM2RAIN
Köppen-Geiger climatic zone	Am	0.56	0.68	0.66	0.68	0.72	0.64	0.61	0.57	0.47	0.28
	Aw	0.47	0.56	0.51	0.56	0.52	0.49	0.53	0.50	0.40	0.34
	BSh	0.51	0.60	0.55	0.62	0.61	0.56	0.63	0.54	0.48	0.41
	BSk	0.55	0.34	0.24	0.29	0.45	0.26	0.43	0.42	0.03	-0.28
	BWh	0.34	0.39	0.51	0.49	0.49	0.39	0.50	0.34	0.42	0.55
	Cfb	0.48	0.46	0.47	0.50	0.54	0.50	0.45	0.50	0.27	0.17
	Csb	0.44	0.57	0.52	0.56	0.54	0.49	0.57	0.47	0.39	0.36
	Cwb	0.49	0.63	0.54	0.61	0.59	0.57	0.60	0.53	0.42	0.35
homogenous rainfall regions	I	0.46	0.68	0.56	0.64	0.61	0.61	0.64	0.54	0.37	0.30
	II	0.57	0.69	0.64	0.69	0.66	0.63	0.67	0.60	0.56	0.42
	III	0.46	0.51	0.48	0.55	0.49	0.42	0.52	0.46	0.35	0.39
	IV	0.55	0.69	0.64	0.67	0.66	0.62	0.67	0.57	0.44	0.33
	V	0.38	0.55	0.33	0.48	0.52	0.36	0.47	0.51	0.33	0.39
	VI	0.28	0.43	0.37	0.38	0.45	0.38	0.38	0.31	0.37	0.16
	VII	0.27	0.47	0.43	0.47	0.46	0.48	0.46	0.32	0.35	0.39
	VIII	0.46	0.45	0.34	0.44	0.48	0.32	0.46	0.41	0.44	0.46
similar seasonal rainfall regimes	RF-A	0.51	0.64	0.56	0.62	0.61	0.55	0.64	0.55	0.39	0.33
	RF-B	0.57	0.69	0.65	0.69	0.68	0.65	0.65	0.61	0.55	0.40
	RF-C	0.32	0.46	0.43	0.46	0.50	0.40	0.44	0.37	0.34	0.36
	RF-D	0.44	0.51	0.47	0.51	0.50	0.42	0.50	0.41	0.39	0.40

CHIRPS, TAMSAT, CMORPH, and MWEP, in order of performance, performed better than all the other products. Among the three products (TAMSAT, CMORHP, and MSEP), CHIRPS performed best in all the rainfall regimes, and the products on the hierarchy of the best products showed changes. Satellite rainfall estimates vary in performance under different rainfall regimes because of factors such as local climate, topography, and elevation(Chen et al., 2021; Romilly and Gebremichael, 2011b). Errors stemming from local rainfall characteristics and subpixel variability could be another influencing factor (Kabite Wedajo et al., 2021).

Overall, the reliability level of the rainfall products varied with climate classification type. In contrast to Köppen-Geiger and rainfall regime climate class-based validation, validation based on homogenous rainfall regions revealed a smaller difference in the 75th and 25th percentiles of box plots for almost all products, which may be associated with a lower possibility of error induced by variations in rainfall patterns in the same class of climate classification. In this case, a smaller change in the performance indicator or KGE value must be considered a significant change. In general, the variation in the choice of best-performing satellite rainfall estimates shows that they are sensitive not only to climate but also to climate classification approaches. This finding implies that climate class-based validation of satellite rainfall estimates needs to consider delineation and validation based on homogenous regions unless rainfall regimes help reduce the errors associated with rainfall characteristics and help identify the best-performing product.

3.4. Validation of rainfall on 12 river basins in Ethiopia

Fig. 8 shows a Tylor diagram demonstrating the accuracy of ten gridded rainfall products for long-term mean monthly rainfall over 12 river basins in Ethiopia. The best-performing SbRE and reanalysis rainfall products approached the purple point (in-situ value), where the standard deviation was zero and the centered normalized mean square error was 1. Accordingly, the common best-performing products for the Abay River Basin, Awash River Basin, Rift Valley River Basin, and Omo Gibe River Basin, in order of performance, were CHIRPS, MSWEP, CMORPH, TAMSAT, and IMERG. Our results were in good agreement with those of previous studies on the same basins(Adane, Hirpa, Lim, et al., 2021; Ayehu et al., 2018b; Dejene et al., 2023; Lakew et al., 2020; Mekonnen et al., 2021). The best performance order of the rainfall products in the Tekeze River Basin also followed the same hierarchy as those in the previous basins did; however, most products presented better correlations, which may be associated with better gauge data quality with smaller missed values than those in the other basins did.

ERA and IMERG were the best-performing products in both the Genale Dawa and Mereb Gash River basins, which is in disagreement with other studies, such as those (Romilly and Gebremichael, 2011b) that prioritizes PERSIAN against CMORPH in the Genale Dawa River Basin. The results imply that there are no commonly best-performing satellite or reanalysis products in all river basins, which implies the necessity of validating rainfall products at each basin or subbasin scale before they are used as decision-support information.

SM2RAIN performed better in the Ogaden, Denakil, Wabi Shebele, and Aysha River Basins, where recurrent drought affects and gauges data-scarce parts of the basin. As all products, except SM2RAIN, are gauge corrected, their performance may decline in areas

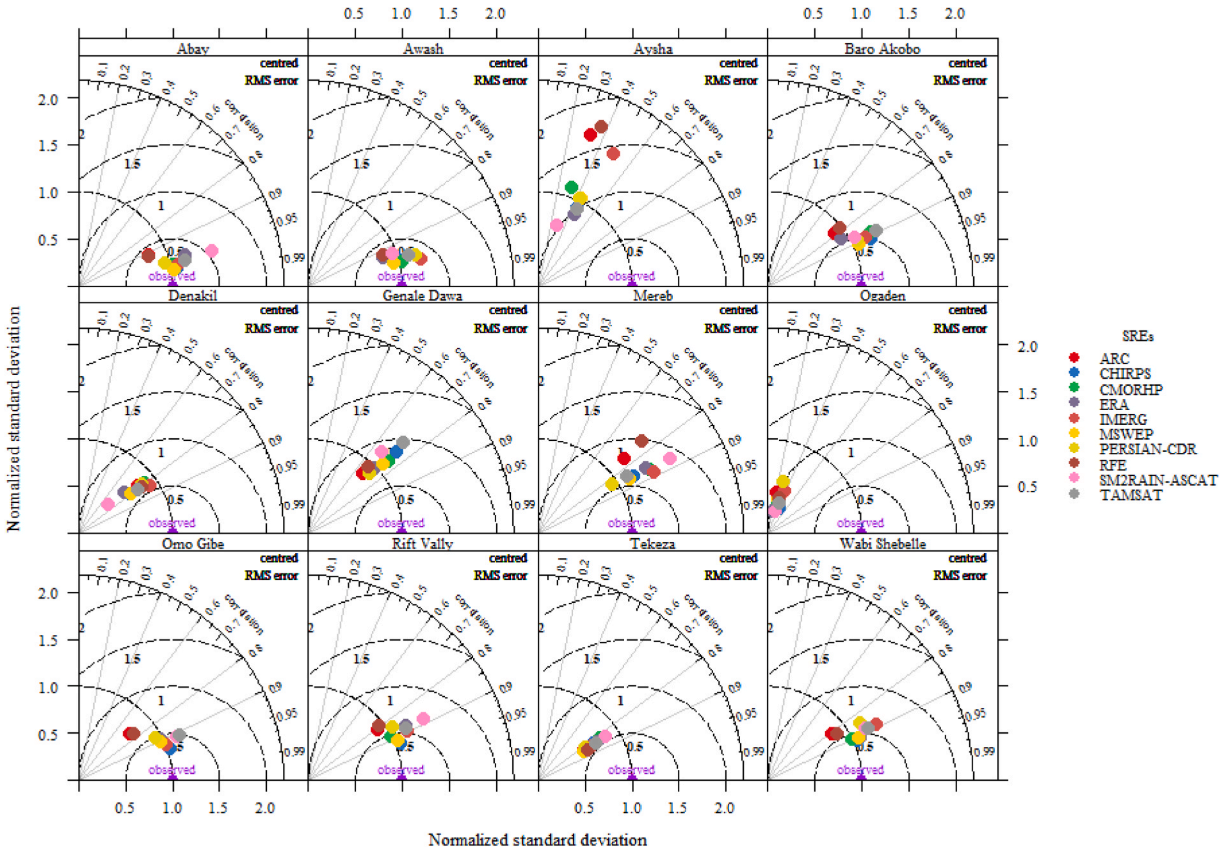

Fig. 8. Taylor diagram shows the monthly statistical comparison for ten SbRE and reanalysis of rainfall products in twelve river basins of Ethiopia.

that do not benefit from gauge observations. In contrast, the SM2RAIN rainfall estimate performed better because it uses a "bottom-up" approach of rainfall estimation based on soil moisture observations and is independent of any satellite rainfall products, which makes it useful in areas where ground observations are scarce or inaccurate(Mosaffa et al., 2023). Additionally, SM2RAIN has been used to improve flood forecasting over 600 basins in Europe, demonstrating its potential for hydrological applications to gauge scarce parts of the eastern Ethiopian basins(Ciabatta et al., 2020).

3.5. Rainfall estimates validation based on the topographic gradient

Previous studies have indicated that topography can influence the accuracy of satellite rainfall estimates in several ways(Bartsotas et al., 2018; Dinku et al., 2007; Mahmoud et al., 2021; Tang et al., 2023). For example, it could be difficult for satellite sensors to detect rainfall accurately in complex topographies because of interactions between atmospheric conditions and topography (Thakur et al., 2019), and topographic masking, which occurs because small-scale terrain features can alter the slope and aspect data of the macroterrain (Gu et al., 2021) and local climate conditions within different topographic extents (Kabite Wedajo et al., 2021).

Fig. 9 shows the comparison of monthly products between SbRE and the reanalysis of rainfall with gauge observations across Ethiopia in different topographic ranges. This result implies a substantial impact of topography on satellite rainfall estimates across Ethiopia. Most products performed better in extremely highlands (above 2500 m) and highlands (between 2000 m and 2500 m). Among the products considered in this study, TAMSAT, CMORPH, and IMERG performed better than the other products did. This result aligns with previous research that revealed that similar products performed well in the central highland part of the country (Ageet et al., 2022; Nile and Bayissa, 2017; Tang et al., 2023; Taye et al., 2023). In contrast, our study findings contradict the findings of other studies that identified CHIRPS and TAMSAT as poor-performing products in the highland part of Ethiopia, particularly in the Upper Blue Nile Basin(Lakew et al., 2020).

The discrepancy in findings could be related to the representation of gauge stations, which could have an impact on the performance of SbRE products within the highland area of Ethiopia(Ayehu et al., 2018). A previous study Thakur et al. (2019) indicated that the spatiotemporal scale at which satellite data can be compared with ground measurements can be a limiting factor in the accuracy of complex topography, as the data may not be fine-grained enough to resolve localized rainfall patterns. As shown in Table 7, one can expect that most gauge-corrected products benefitted more from dense gauges in areas with extremely highland and highland topographic range coverage, where 10 % and 6 % of the country was represented by 117 and 53 gauge stations, respectively. Furthermore,

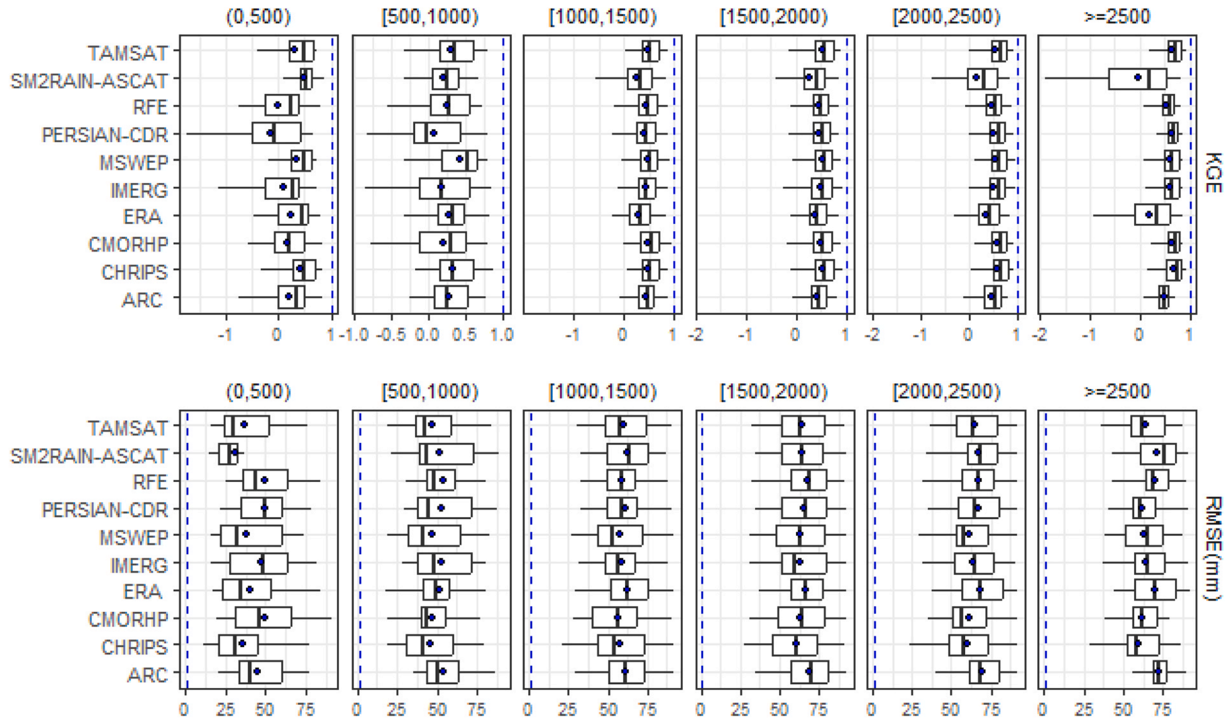

Fig. 9. Comparison between monthly SbRE and reanalysis rainfall estimates and the corresponding in-situ observations using KGE and RMSE for different elevation zones in Ethiopia. The dashed blue line indicates the optimal values for each performance metric. The right and left lines of the boxplot represent the 75th and 25th percentiles, respectively, whereas the middle vertical line indicates the median value. Black dots indicate the mean values of each performance metric.

Table 7
Topographic classification and the performance (KGE) of SbRE across each topographic range of Ethiopia.

Elevation (m.a.s.l)	ARC	CHIRPS	CMORPH	ERA	IMEGR	MSWEP	PERSIAN-CDR	RFE	SM2RAIN	TAMSAT
(−125,500)	0.21	0.38	0.13	0.21	0.09	0.34	−0.16	0.00	0.50	0.30
[500,1000)	0.25	0.33	0.31	0.34	0.17	0.52	−0.03	0.23	0.25	0.35
[1000,1500)	0.45	0.51	0.54	0.31	0.42	0.51	0.45	0.47	0.33	0.51
[1500,2000)	0.47	0.58	0.51	0.42	0.51	0.55	0.53	0.49	0.41	0.57
[2000,2500)	0.52	0.64	0.63	0.42	0.60	0.63	0.60	0.55	0.29	0.64
> =2500	0.51	0.75	0.70	0.35	0.65	0.65	0.67	0.59	0.18	0.71

the percentage of missing data (Fig. 2) could have an impact on the performance and related choices of rainfall estimation products.

The results in the lowland area (Fig. 9 and Table 7) also revealed that SM2RAIN, CHIRPS, and MSWEP, in order of performance, performed better in the extremely lowest topographic areas (between 0 and 500 m), and for the topographic areas between 500 m and 1000 m, the performance of MSWEP, TAMSAT, and ERA, in order of performance, performed better, with the highest median value of KGE, which extends between 0.63 and 0.65, and the lowest RMSE, which ranges between 26 mm and 33 mm. In contrast, the products of PERSIAN-CDR, RFE, and IMERG performed poorly on the extremely low topography (between 0 and 500 m) and lowest (500 m to 1000 m), with 14.4 % and 28.7 % coverage of the country area, respectively.

3.6. Validation only on recurrent drought-affected regions of Ethiopia

Out of the area affected by recurrent drought in Ethiopia (Fig. 2F), the upper half receives both MAM and JJAS rainfall or is categorized as rainfall regime-A, and the lower half receives both MAM and SON rainfall or is categorized under rainfall regime-C (see Fig. 2C). To understand the comparative reliability of rainfall products for drought monitoring, they were validated by comparing the correlation coefficients between the gauge and SbRE products by grouping them into three categories.

The top two panels (without*) of the scatter plot in Fig. 10 show the correlation between the rainfall estimate products and ground observations for the period between 2001 and 2020 for all months of the recurrent drought-affected regions in Ethiopia. The results revealed that CHIRPS (R=0.65) outperformed all the other products, followed by three products (MSWEP, TAMSAT, and IMERG), with similar correlation coefficients (R=0.64). These findings align with those of previous studies that identified the CHIRPS as the best

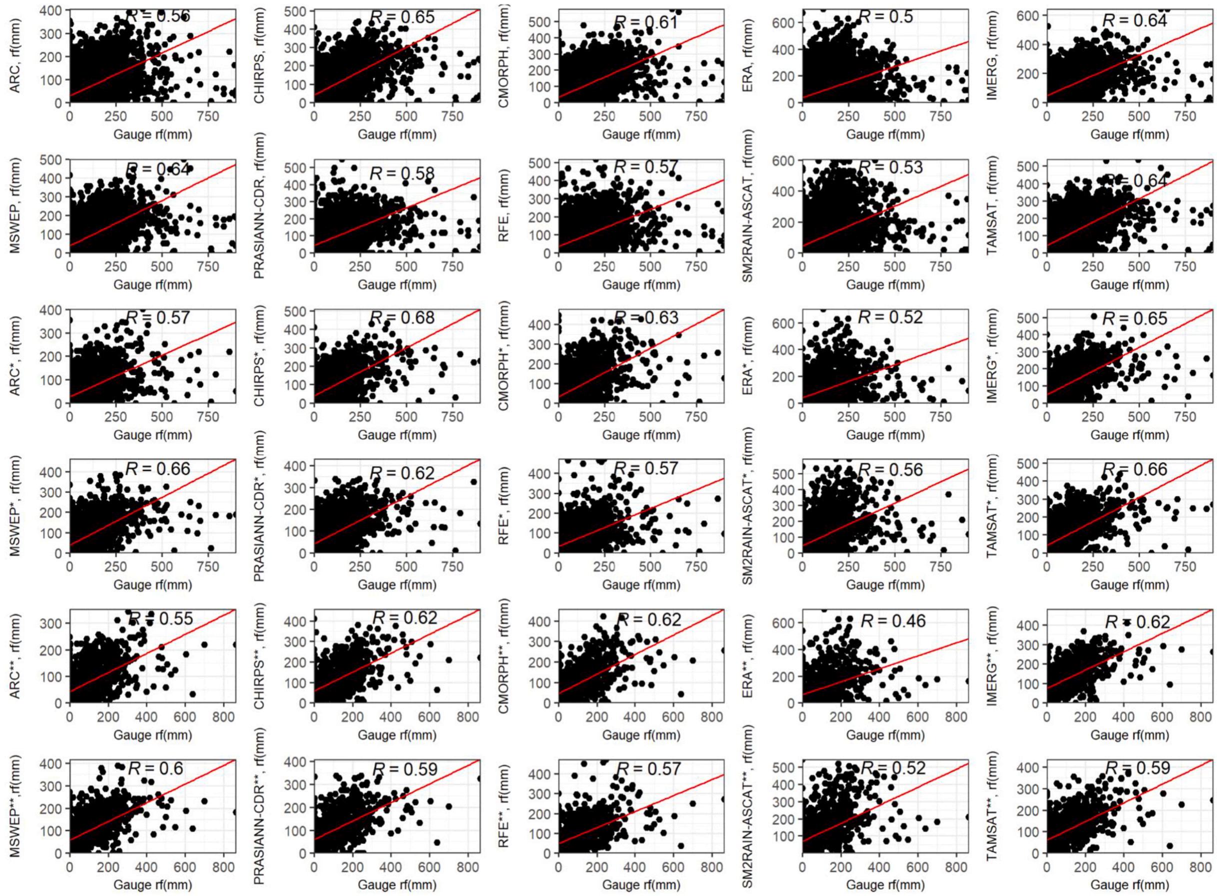

Fig. 10. Scatter plot of ten SbRE and reanalysis of rainfall products in replicating recurrent drought-affected regions of Ethiopia. The top two panels (without *) represent the monthly mean rainfall for the period between 2001 and 2020, the middle two panels represent monthly rainfall for the seven drought years (the year 2002, 2003, 2006, 2011,2015, 2016, and 2017), and the bottom two panels(with **) show the wet season rainfall for the seven drought years.

satellite rainfall estimation product for meteorological drought monitoring in various regions of Ethiopia(Bayissa et al., 2017; Lemma et al., 2022).

The middle two panels (with*) of the scatter plot in Fig. 10 show the monthly correlation between SbRE and the reanalysis rainfall estimate products and the gauge for only the seven major drought-affected years (the years 2002, 2003, 2006, 2011, 2015, 2016, and 2017) within the study period between 2001 and 2020. The results showed that the CHIRPS was still better correlated with ground observations (R=0.68) than the other products were and was followed by a comparable correlation between ground observations and the rainfall products MSWEP and TAMSAT, with a correlation coefficient of R= 0.66.

The bottom two panels (with**) of the scatter plot in Fig. 10 show the monthly correlation between SbRE and ground observations for the main rainy or wet season of the seven drought years (region and season A= MAM and JJAS, and region C= MAM and SON). The results revealed that CHIRPS, CMORPH, and IMERG performed better than the other products did and presented a comparative correlation (R=0.62). This finding is also aligned with a study that evaluated satellite rainfall estimate product drought capture ability on the basis of a drought index focusing on three wet seasons in Ethiopia, Belg (MAM), Autumn (SON), and Kiremt (JJAS), which identified the CHIRPS as the best-performing product in all three seasons(Degefu and Bewket, 2023).

Among the three categories of temporal resolution, CHIRPS, MEWEP, TAMSAT, and IMERG showed better correlations with ground observations in recurrent drought-affected regions of Ethiopia. This result is similar to previous findings, which indicate that the accuracy of satellite rainfall estimates could vary under wet, drought, and normal conditions in the same region (Qureshi et al., 2022). This finding is also an indication for identifying reliable products for drought monitoring on the basis of historical drought years, and the wet seasons of drought years may not help reach a consistent and conclusive finding.

3.7. Suggested products for various applications in Ethiopia

The four spatial maps in Fig. 11 illustrate a summary of the four suggested rainfall products, in order of performance, for the application of climatology, drought monitoring, water resources (or general hydrology), and flood monitoring. The first two sectors

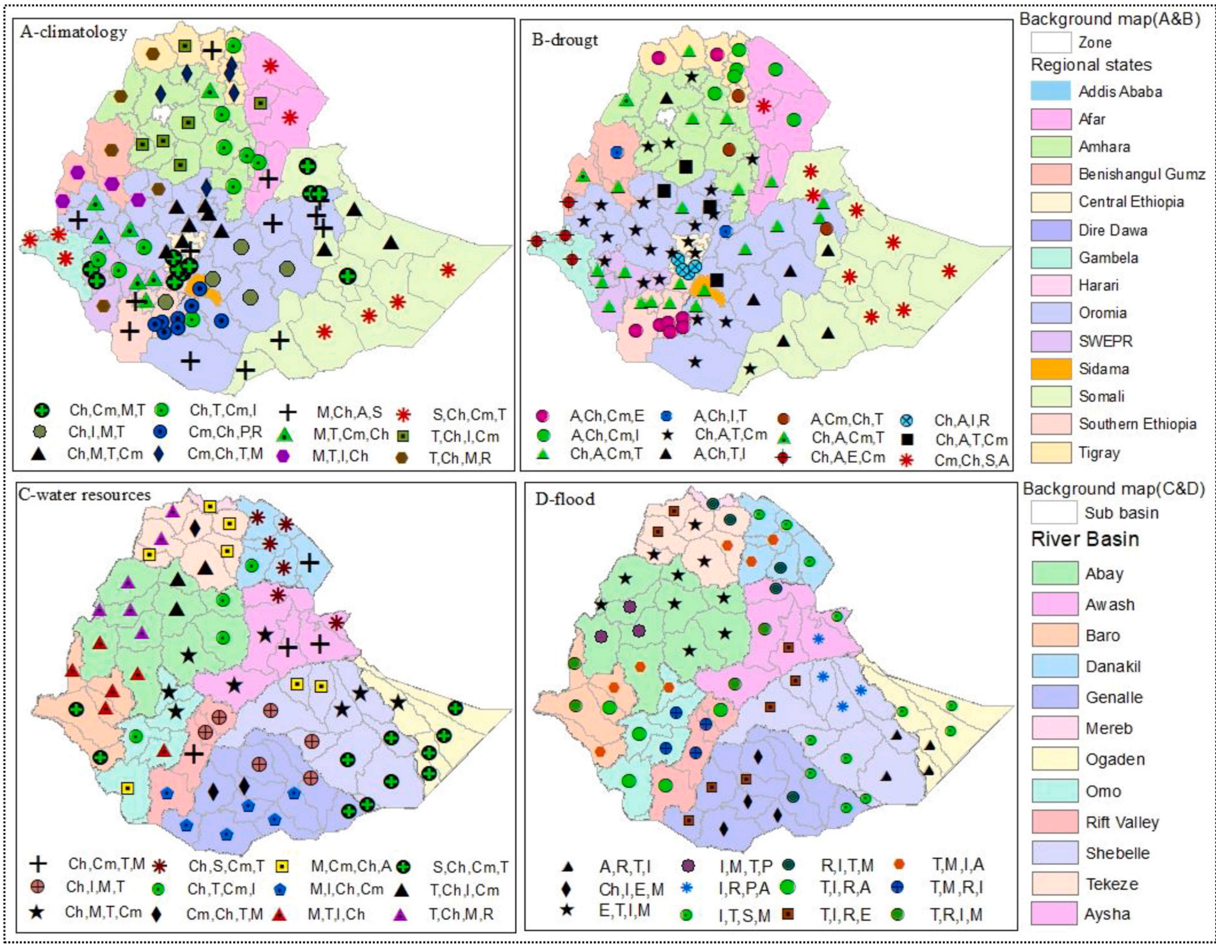

Fig. 11. Spatial representation of the suggested rainfall products, in order of performance, for the monitoring and application of rainfall climatology (Fig. 11A), drought monitoring (Fig. 11B), water resources or general hydrology (Fig. 11C) and flood monitoring (Fig. 11D) across Ethiopia. The background map representations for maps A and B are the regional state administrative boundaries, whereas the background representations for maps C and D are river basins in Ethiopia. Note: −1 Symbol representation of rainfall products: A-ARC; Ch-CHIRPS; Cm-CMORPH; E-ERA; I-IMERG; M-MSWEP; P-PERSIANN-CDR; R-RFE; T-TAMSAT; S-SM2RAIN 2 Ethiopia is divided into 14 regional states and 2 chartered cities, which are also subdivided into 92 zonal administrative boundaries according to the 2024 reports of OCHA-ETHIOPAI. Climatological and drought monitoring activities are usually communicated at administrative boundaries in Ethiopia. 3 In this map, the 12 river basins of Ethiopia were divided into 76 subbasins by modifying the HydroBASINS level-6 classification (Lehner and Grill, 2013). General hydrological and flood monitoring information usually follows various classes of basin divisions. 4 The choice of rainfall products for flood and drought monitoring and applications was heavily impacted by their ability to detect rainfall > 30 mm and rainfall < 1 mm, respectively, on a daily timescale. The dataset suggested for climatological analysis and water resources (general hydrology) was selected on the basis of the mean and KGE values of the monthly data.

(Fig. 11A-climatology and Fig. 11B-drought) are suggested at the zonal administrative boundary, and the preceding two sectors (Fig. 11C-water resources and Fig. 11D-flood) are suggested at the subbasin level. In most cases, the difference in the top best-performing products is marginal; hence, a suggestion for reliable products was made by considering the dominance of the product ranking in the 50 spatial scales considered in this study.

The results of multiple spatial-scale validations of rainfall products revealed major variability in performance across Ethiopia (Fig. 11). For example, for climatological applications, CHIRPS, MSWEP, and CMORPH were identified as the best representative products, in order of performance, for more than 92 % of the 50 spatial scales. For flood monitoring applications, IMERG, TAMSAT, and RFE were identified (>86 % of the 50 spatial scales) as reliable products. For drought monitoring, ARC and CHIRPS were the dominant (>95 % of the 50 spatial scales) reliable products. Similarly, CHIRPS, MSWEP, and TAMSAT were identified (> 82 % of the 50 spatial scales) as reliable products for the analysis of water resources and general hydrology. In general, performance can vary according to region, climate zone, topography, and other factors. Accordingly, all hydrophysical impacts can affect the reliability of rainfall products for various applications.

4. Limitations of the study

Each satellite rainfall estimate product has its caveats that are induced by the limitations of the individual sensors utilized, even though most satellite rainfall estimate products may use combined inputs from multiple sensors, such as infrared, visible, active/passive, and gauge sensors. For example, because of sensor limitations in capturing the orographic enhancement of rainfall, SbRE products could miss 20–40 % of the total rainfall in mountainous regions (Asfaw et al., 2023; Cha et al., 2014; Taye et al., 2023).

This study employed a pixel—point evaluation approach by comparing gridded SbRE and reanalysis rainfall estimates with point ground gauge observations, which may introduce uncertainty due to the comparison of spatially different datasets and point ground observations may not capture the variability in rainfall within a pixel of gridded data.

These findings could be affected by the quality, quantity, analysis approach, and spatial distribution of the gauge data. For example, the percentage of missing gauge observation data extends to 30 % for some ground observation point data within the study period. Daily missing data could affect the representation of subsequent monthly and yearly data while aggregating the monthly and annual resolution performance evaluation findings. Moreover, the spatial representation of gauge data is not aligned with the World Meteorological Organization (WMO) standards in some parts of the country. For example, the density of meteorological stations is sparsely distributed in less populated areas of the southern and southeastern parts of the country and downstream of every river basin, which may limit the fair spatial evaluation of gridded data in each part of the country.

The validation findings did not consider the rainfall variability within the region of the boundaries classified for the analysis. For example, the performance of each product varied within the river basins of Ethiopia, namely, the Awash, Abay, Rift Valley, and Genalle Dawa River Basins, due to multiple factors, including variations in the topographic gradient compared to those upstream and downstream. However, in this study, a part of the validation analysis was conducted without considering spatial differences.

5. Conclusion

This study aimed to conduct a comprehensive validation of the accuracy of ten long-years satellite and reanalysis rainfall estimate products (CMORHP v2.0, IMERG v06B, RFE v2.0, ARC v2.0, CHIRPS v2.0, PERSIAN-CDR, SM2RAIN-ASCAT, TAMSAT v3.1, MSWEP v2.8, and ERA 5) for the period from 2001–2020 by comparing 430 points of in-situ data across Ethiopia. To achieve this objective, five continuous and six categorical performance metrics were introduced. A comprehensive evaluation was conducted at multiple spatial (national scale, elevation, basin, multiple climate classification classes, and drought zones) and temporal (daily, monthly, seasonal, and annual) scales. The key findings of this study are as follows.

- None of the ten rainfall products were steadily performed at all spatial and temporal resolutions considered in this study. In general, all products performed poorly and overestimated daily rainfall; however, the CMORHP, MSWEP, IMERG, and CHIRPS, in order of performance, ranked relatively better than the other datasets at the daily time scale. The CHIRPS, MSWEP, CMORHP, and IMERG rainfall estimation products, in order of performance, attained the optimal values better than all the other products did at both the monthly and annual scales. For all temporal scales, the TAMSAT product yielded subpar results, although high-resolution data were obtained compared to the remaining nine products. This finding indicates that more reliable products cannot necessarily be obtained by increasing their resolution.
- Almost all the products perform well in detecting no rainfall, but their performance decreases as the rainfall rate increases. Among these products, ARC, CHIRPS, and TAMSAT, in order of performance, excel in detecting "no rain" across Ethiopia, making them suitable for dry spell or drought monitoring across Ethiopia. In contrast, IMERG, RFE, and CMORHP are more effective at capturing high-intensity rainfall, which results in better products for flood-related analysis. However, the performance of the top selected products for drought and flood monitoring varied from one location to another.
- The performance of rainfall products is heavily affected by climate, and the choice of best-performing products is sensitive to climate classification approaches. On the basis of the Köppen-Geiger climatic zone classification, CHIRPS and TAMSAT performed best in tropical climates, and MSEP and TAMSAT performed best in arid climates. CHIRPS, CMORPH, and MSWEP performed better in regions with homogenous rainfall. The performance validation based on similar seasonal rainfall patterns revealed that CHIRPS performed best in all rainfall regimes, but the preceding best products varied among TAMSAT, CMORPH, and MSWEP in different seasonal rainfall regimes. The results indicate the importance of reasonable choices in climate classification approaches for validating rainfall products.
- The validation results show that elevation has a significant effect on the performance of satellite-based rainfall products in a country such as Ethiopia, which has a very rugged and rigid topography. For example, at extremely low elevations ($<$500 m), SM2RAIN and CHIRPS performed better, depending on the gauge density. MSWEP at elevations ranging between 500 m and 1000 m, CMORHP at elevations between 1000 m and 1500 m, and both CHIRPS and TAMSAT perform better at elevations $>$ 2000 m.

The results of this study offer several selected rainfall products for specific localities or national scales for climatological, drought monitoring, flood risk, and water resources management in Ethiopia. For example, CHIRPS and MSWEP are relatively better products that represent the majority of the country's climatological characteristics, whereas IMERG and TAMSAT are suitable for flood monitoring. The ARC and CHIRPS are useful for drought monitoring, whereas the CHIRPS and MSWEP are useful for water resource analysis. In general, the study revealed that the characteristics of satellite-based rainfall and reanalysis rainfall products vary with space and time, which implies the importance of locational performance in choosing rainfall products for various applications.

CRediT authorship contribution statement

Desta Yoseph Wodebo: Writing – original draft, Visualization, Validation, Software, Methodology, Investigation, Formal analysis, Data curation, Conceptualization. **Assefa M Melesse:** Writing – review & editing, Validation, Supervision, Methodology, Conceptualization. **Tekalegn Ayele Woldesenbet:** Writing – review & editing, Validation, Supervision, Methodology, Conceptualization. **Kirubel Mekonnen:** Writing – review & editing, Validation, Software, Methodology, Data curation, Conceptualization. **Ahmed Amdihun:** Writing – review & editing, Validation. **Diriba Korecha:** Writing – review & editing, Validation. **Hailay Zeray Tedla:** Writing – review & editing, Validation, Data curation. **Gerald Corzo:** Writing – review & editing, Validation. **Asaminew Teshome:** Writing – review & editing, Validation.

Declaration of Competing Interest

The authors declare that they have no known competing financial interests or personal relationships that could have appeared to influence the work reported in this paper.

Acknowledgments

We acknowledge the Ethiopian Meteorological Institute (EMI) for providing daily rainfall data. We are grateful to the data providers of all satellite-based and reanalysis rainfall estimates, digital elevation models (DEM), administrative boundaries, and GIS shapefiles considered in this study. The first author would like to acknowledge Ethiopian Construction Design and Supervision Works Corporation, Water and Energy Design and Supervision Sector, its former CEO (Negede Abate) and staff memebers for encouraging similar studies to be conducted to tackle hydromet datascarcity challenges in Ethiopia's DRM and water resources sectors.

Data availability

Data will be made available on request.

References

Ababa, A., 2021. Natl. Meteorol. Agency Revis. Meteorol. Station Netw. Master Plan Revis. Meteorol. Station Netw. Master Plan Prep. Tech. Comm.

Abate, N.T., Banda, L.B., Resources, N., Education, S., 2020. *Model. Distrib. four-Bird. Species Clim. Change Eff. have already Start. manifesting Differ. taxa (Chen Et. al., 2011; Will. shift their Geogr. Distrib. Clim. Change they Track. Sept.* 0–17.

Abera, W., Brocca, L., Rigon, R., 2016. Comparative evaluation of different satellite rainfall estimation products and bias correction in the Upper Blue Nile (UBN) basin. *Atmos. Res.*, *178–179* 471–483. https://doi.org/10.1016/j.atmosres.2016.04.017.

Adane, G.B., Hirpa, B.A., Gebru, B.M., Song, C., Lee, W.K., 2021. Integrating satellite rainfall estimates with hydrologicalwater balance model: Rainfall-runoff modeling in awash river basin, ethiopia. Water (Switz.) 13 (6). https://doi.org/10.3390/w13060800.

Adane, G.B., Hirpa, B.A., Lim, C.H., Lee, W.K., 2021. Evaluation and comparison of satellite-derived estimates of rainfall in the diverse climate and terrain of central and northeastern ethiopia. Remote Sens. 13 (7). https://doi.org/10.3390/rs13071275.

Ageet, S., Fink, A.H., Maranan, M., Diem, J.E., Hartter, J., Ssali, A.L., Ayabagabo, P., 2022. Validation of Satellite Rainfall Estimates over Equatorial East Africa. J. Hydrometeorol. 23 (2), 129–151. https://doi.org/10.1175/JHM-D-21-0145.1.

Aghakouchak, A., Mehran, A., Norouzi, H., Behrangi, A., 2012. Systematic and random error components in satellite precipitation data sets. Geophys. Res. Lett. 39 (9), 3–6. https://doi.org/10.1029/2012GL051592.

Alghafli, K., Ali, A.M., Shi, X., Sloan, W., Obeid, A.A.A., 2023. Journal of Hydrology: Regional Studies Evaluation of runoff estimation from GRACE coupled with different meteorological gridded products over the Upper Blue Nile Basin. J. Hydrol.: Reg. Stud. 50, 101545. https://doi.org/10.1016/j.ejrh.2023.101545.

Alhamshry, A., Ayele, F.A., Yasuda, H., Kimura, R., Shimizu, K., 2020. Seasonal Rainfall Variability in Ethiopia and Its. Water 12 (55), 1–19.

Ali, M.H., Popescu, I., Jonoski, A., Solomatine, D.P., 2023. Remote Sensed and/or Global Datasets for Distributed Hydrological Modelling: A Review. Remote Sens. 15 (6), 1–43. https://doi.org/10.3390/rs15061642.

Almaw, A., Yasuda, H., Shimizu, K., Ibaraki, Y., 2018. Evaluation of satellite rainfall estimates over the Lake Tana basin at the source region of the Blue Nile River. Atmos. Res. 212 (May), 43–53. https://doi.org/10.1016/j.atmosres.2018.05.009.

Asfaw, W., Rientjes, T., Haile, A.T., 2023. Blending high-resolution satellite rainfall estimates over urban catchment using Bayesian Model Averaging approach. J. Hydrol.: Reg. Stud. 45, 101287. https://doi.org/10.1016/j.ejrh.2022.101287.

Ayat, H., Evans, J.P., Behrangi, A., 2021. How do different sensors impact IMERG precipitation estimates during hurricane days? *Remote Sens. Environ.* 259. https://doi.org/10.1016/j.rse.2021.112417.

Ayehu, G.T., Tadesse, T., Gessesse, B., Dinku, T., 2018a. Validation of new satellite rainfall products over the Upper Blue Nile Basin, Ethiopia. Atmos. Meas. Tech. 11 (4), 1921–1936. https://doi.org/10.5194/amt-11-1921-2018.

Ayehu, G.T., Tadesse, T., Gessesse, B., & Dinku, T. (2018b). Validation of new satellite rainfall products over the Upper Blue Nile Basin, Ethiopia. 1921–1936.

Bai, L., Shi, C., Li, L., Yang, Y., Wu, J., 2018. Accuracy of CHIRPS satellite-rainfall products over mainland China. Remote Sens. 10 (3). https://doi.org/10.3390/rs10030362.

Bajracharya, S.R., Shrestha, M.S., & Shrestha, A.B. (n.d.). *Assessment of high-resolution satellite rainfall estimation products in a streamflow model for flood prediction in the Bagmati basin, Nepal*. https://doi.org/10.1111/jfr3.12133.

Bartsotas, N.S., Anagnostou, E.N., Nikolopoulos, E.I., Kallos, G., 2018. Investigating Satellite Precipitation Uncertainty Over Complex Terrain. J. Geophys. Res.: Atmospheres 123 (10), 5346–5359. https://doi.org/10.1029/2017JD027559.

Battaglia, A., Kollias, P., Dhillon, R., Lamer, K., Khairoutdinov, M., Watters, D., 2020. Mind the gap-Part 2: Improving quantitative estimates of cloud and rain water path in oceanic warm rain using spaceborne radars. Atmos. Meas. Tech. 13 (9), 4865–4883. https://doi.org/10.5194/amt-13-4865-2020.

Bayissa, Y., Tadesse, T., Demisse, G.B., Shiferaw, A.S., 2017. *Eval. Satell. -Based Rainfall Estim. Appl. Monit. Meteorol. Drought Up. Blue Nile Basin, Ethiop. June.* https://doi.org/10.3390/rs9070669.

Beck, H.E., Zimmermann, N.E., McVicar, T.R., Vergopolan, N., Berg, A., Wood, E.F., 2018. Present and future köppen-geiger climate classification maps at 1-km resolution. Sci. Data 5, 1–12. https://doi.org/10.1038/sdata.2018.214.

Bertini, C., Buonora, L., Ridolfi, E., Russo, F., Napolitano, F., 2020. On the use of satellite rainfall data to design a dam in an ungauged site. Water (Switz.) 12 (11), 1–20. https://doi.org/10.3390/w12113028.

Bhuiyan, M.A.E., Nikolopoulos, E.I., Anagnostou, E.N., 2019. Machine learning–based blending of satellite and reanalysis precipitation datasets: A multiregional tropical complex terrain evaluation. J. Hydrometeorol. 20 (11), 2147–2161. https://doi.org/10.1175/JHM-D-19-0073.1.

Bitew, M.M., Gebremichael, M., 2011. Assess. Satell. Rainfall Prod. Streamflow Simul. Medium Watersheds Ethiop. Highl. 1147–1155. https://doi.org/10.5194/hess-15-1147-2011.

Bonnema, M., Sikder, S., Miao, Y., Chen, X., Hossain, F., Ara Pervin, I., Mahbubur Rahman, S.M., Lee, H., 2016. Understanding satellite-based monthly-to-seasonal reservoir outflow estimation as a function of hydrologic controls. Water Resour. Res. 52 (5), 4095–4115. https://doi.org/10.1002/2015WR017830.

Borgomeo, E., Vadheim, B., Woldeyes, F.B., Alamirew, T., Tamru, S., Charles, K.J., Kebede, S., Walker, O., 2018. The Distributional and Multi-Sectoral Impacts of Rainfall Shocks: Evidence From Computable General Equilibrium Modelling for the Awash Basin, Ethiopia. Ecol. Econ. 146 (April 2017), 621–632. https://doi.org/10.1016/j.ecolecon.2017.11.038.

Brocca, L., Filippucci, P., Hahn, S., Ciabatta, L., Massari, C., Camici, S., Schüller, L., Bojkov, B., & Wagner, W. (2019). SM2RAIN – ASCAT (2007 – 2018): global daily satellite rainfall data from ASCAT soil moisture observations. 3405563(August), 1583–1601.

Burdanowitz, J., Nuijens, L., Stevens, B., Klepp, C., 2015. Evaluating light rain from satellite- and ground-based remote sensing data over the subtropical North Atlantic. J. Appl. Meteorol. Climatol. 54 (3), 556–572. https://doi.org/10.1175/JAMC-D-14-0146.1.

Cha, Y., Park, S.S., Kim, K., Byeon, M., Stow, C.A., 2014. Water Resour. Res. 5375–5377. https://doi.org/10.1002/2013WR014979.Reply.

Chen, Y., Duan, J., An, J., Liu, H., Görsdorf, U., Berger, F.H., 2021. Satellite estimates and subpixel variability of rainfall in a semi-arid grassland. Atmos. Ocean. Sci. Lett. 14 (5), 100055. https://doi.org/10.1016/j.aosl.2021.100055.

Cheung, W.H., Senay, G.B., Singh, A., 2008. Trends and spatial distribution of annual and seasonal rainfall in Ethiopia. Int. J. Climatol. 28 (13), 1723–1734. https://doi.org/10.1002/joc.1623.

Ciabatta, L., Camici, S., Massari, C., Filippucci, P., Hahn, S., Wagner, W., Brocca, L., 2020. Soil moisture and precipitation: The SM2RAIN algorithm for rainfall retrieval from satellite soil moisture. Adv. Glob. Change Res. 69, 1013–1027. https://doi.org/10.1007/978-3-030-35798-6_27.

Degefu, M.A., Bewket, W., 2023. Drought monitoring performance of global precipitation products in three wet seasons in Ethiopia: Part I—Quasi-objective examination. Meteorol. Appl. 30 (4), 1–28. https://doi.org/10.1002/met.2143.

Dejene, I.N., Wedajo, G.K., Bayissa, Y.A., Abraham, A.M., Cherinet, K.G., 2023. Satell. Rainfall Perform. Eval. Appl. … 2023 Satell. Rainfall Perform. Eval. Appl. *Nat. Hazards* (Issue August). Springe Neth. https://doi.org/10.1007/s11069-023-06127-2.

Dinku, T., 2019. Challenges with availability and quality of climate data in Africa. November. https://doi.org/10.1016/B978-0-12-815998-9.00007-5.

Dinku, T., Ceccato, P., Grover-Kopec, E., Lemma, M., Connor, S.J., Ropelewski, C.F., 2007. Validation of satellite rainfall products over East Africa's complex topography. Int. J. Remote Sens. 28 (7), 1503–1526. https://doi.org/10.1080/01431160600954688.

Dinku, T., Funk, C., Peterson, P., Maidment, R., Tadesse, T., Gadain, H., Ceccato, P., 2018. Validation of the CHIRPS satellite rainfall estimates over eastern Africa. Q. J. R. Meteorol. Soc. 144 (June 2017), 292–312. https://doi.org/10.1002/qj.3244.

Dinku, T., Funk, C., Peterson, P., Maidment, R., Tadesse, T., 2018. *Valid. CHIRPS Satell. Rainfall Estim. East. Jan.* 292–312. https://doi.org/10.1002/qj.3244.

Dumont, M., Saadi, M., Oudin, L., Lachassagne, P., Nugraha, B., Fadillah, A., Bonjour, J.L., Muhammad, A., Hendarmawan, Dörfliger, N., Plagnes, V., 2022. Assessing rainfall global products reliability for water resource management in a tropical volcanic mountainous catchment. J. Hydrol.: Reg. Stud. 40 (December 2021). https://doi.org/10.1016/j.ejrh.2022.101037.

Faccenna, C., Glišović, P., Forte, A., Becker, T.W., Garzanti, E., Sembroni, A., Gvirtzman, Z., 2019. Role of dynamic topography in sustaining the Nile River over 30 million years. Nat. Geosci. 12 (12), 1012–1017. https://doi.org/10.1038/s41561-019-0472-x.

Fich, E.A. (2022). Drought Response. 2022(24 November 2011). ⟨http://www.sa.gov.au/subject/Water,+energy+and+environment/Water/Drought+response⟩.

Filippucci, P., Brocca, L., Quast, R., Ciabatta, L., Saltalippi, C., Wagner, W., Tarpanelli, A., 2022. High-resolution (1 km) satellite rainfall estimation from SM2RAIN applied to Sentinel-1: Po River basin as a case study. Hydrol. Earth Syst. Sci. 26 (9), 2481–2497. https://doi.org/10.5194/hess-26-2481-2022.

Funk, C.C., Peterson, P.J., Landsfeld, M.F., Pedreros, D.H., Verdin, J.P., Rowland, J.D., Romero, B.E., Husak, G.J., Michaelsen, J.C., Verdin, A.P., 2014. A Quasi-Global Precipitation Time Series for Drought Monitoring. U. S. Geol. Surv. Data Ser. 832, 4.

Funk, C., Peterson, P., Landsfeld, M., Pedreros, D., Verdin, J., Shukla, S., Husak, G., Rowland, J., Harrison, L., Hoell, A., Michaelsen, J., 2015. The climate hazards infrared precipitation with stations - A new environmental record for monitoring extremes. Sci. Data 2, 1–21. https://doi.org/10.1038/sdata.2015.66.

Garba, J.N., Diasso, U.J., Waongo, M., Sawadogo, W., Daho, T., 2023. Performance evaluation of satellite-based rainfall estimation across climatic zones in Burkina Faso. *0123456789* Theor. Appl. Climatol.. https://doi.org/10.1007/s00704-023-04593-z.

Gebere, S.B., Alamirew, T., Merkel, B.J., Melesse, A.M., 2015. Performance of high resolution satellite rainfall products over data scarce parts of eastern ethiopia. Remote Sens. 7 (9), 11639–11663. https://doi.org/10.3390/rs70911639.

Gebrechorkos, S.H., Hülsmann, S., Bernhofer, C., 2018. Evaluation of multiple climate data sources for managing environmental resources in East Africa. Hydrol. Earth Syst. Sci. 22 (8), 4547–4564. https://doi.org/10.5194/hess-22-4547-2018.

Gebremicael, T., Mohamed, Y., van der Zaag, P., Berhe, A., Haile, G., Hagos, E., Hagos, M., 2017. Comparison and validation of eight satellite rainfall products over the rugged topography of Tekeze-Atbara Basin at different spatial and temporal scales. Hydrol. Earth Syst. Sci. Discuss.

Getirana, A.C.V., Espinoza, J.C.V., Ronchail, J., Rotunno Filho, O.C., 2011. Assessment of different precipitation datasets and their impacts on the water balance of the Negro River basin. J. Hydrol. 404 (3–4), 304–322. https://doi.org/10.1016/j.jhydrol.2011.04.037.

Goshime, D.W., Absi, R., Ledésert, B., 2019. Evaluation and bias correction of CHIRP rainfall estimate for rainfall-runoff simulation over Lake Ziway Watershed, Ethiopia. Hydrology 6 (3). https://doi.org/10.3390/hydrology6030068.

Gu, W., Zhu, X., Meng, X., Qiu, X., 2021. Res. Influ. Small-Scale Terrain Precip. 1–15.

Gumindoga, W., Rientjes, T.H.M., Haile, A.T., Makurira, H., Reggiani, P., 2016. Bias correction schemes for CMORPH satellite rainfall estimates in the Zambezi River Basin. Hydrol. Earth Syst. Sci. Discuss. 0 (February), 1–36. https://doi.org/10.5194/hess-2016-33.

Gummadi, S., Dinku, T., Shirsath, P.B., Kadiyala, M.D.M., 2022. Evaluation of multiple satellite precipitation products for rainfed maize production systems over Vietnam. Sci. Rep. 12 (1), 1–18. https://doi.org/10.1038/s41598-021-04380-8.

He, K., Zhao, W., Brocca, L., Quintana-Seguí, P., 2023. SMPD: A soil moisture-based precipitation downscaling method for high-resolution daily satellite precipitation estimation. Hydrol. Earth Syst. Sci. 27 (1), 169–190. https://doi.org/10.5194/hess-27-169-2023.

Hersbach, H., Bell, B., Berrisford, P., Hirahara, S., Horányi, A., Muñoz-Sabater, J., Nicolas, J., Peubey, C., Radu, R., Schepers, D., Simmons, A., Soci, C., Abdalla, S., Abellan, X., Balsamo, G., Bechtold, P., Biavati, G., Bidlot, J., Bonavita, M., Thépaut, J.N., 2020. The ERA5 global reanalysis. Q. J. R. Meteorol. Soc. 146 (730), 1999–2049. https://doi.org/10.1002/qj.3803.

Hinge, G., Hamouda, M.A., Long, D., Mohamed, M.M., 2022. Hydrologic utility of satellite precipitation products in flood prediction: A meta-data analysis and lessons learnt. J. Hydrol. 612 (PA), 128103. https://doi.org/10.1016/j.jhydrol.2022.128103.

Hordofa, A.T., Leta, O.T., Alamirew, T., Kawo, N.S., Chukalla, A.D., 2021. Performance evaluation and comparison of satellite-derived rainfall datasets over the Ziway lake basin, Ethiopia. Climate 9 (7). https://doi.org/10.3390/cli9070113.

Hossain, F., Huffman, G.J., 2008. Investigating error metrics for satellite rainfall data at hydrologically relevant scales. J. Hydrometeorol. 9 (3), 563–575. https://doi.org/10.1175/2007JHM925.1.

Joyce, R.J., Janowiak, J.E., Arkin, P.A., Xie, P., 2004. CMORPH: A method that produces global precipitation estimates from passive microwave and infrared data at high spatial and temporal resolution. J. Hydrometeorol. 5 (3), 487–503. https://doi.org/10.1175/1525-7541(2004)005< 0487:CAMTPG> 2.0.CO;2.

Kabite Wedajo, G., Kebede Muleta, M., Gessesse Awoke, B., 2021. Performance evaluation of multiple satellite rainfall products for Dhidhessa River Basin (DRB), Ethiopia. Atmos. Meas. Tech. 14 (3), 2299–2316. https://doi.org/10.5194/amt-14-2299-2021.

Katiraie-Boroujerdy, P.S., Naeini, M.R., Asanjan, A.A., Chavoshian, A., Hsu, K. lin, Sorooshian, S., 2020. Bias correction of satellite-based precipitation estimations using quantile mapping approach in different climate regions of Iran. Remote Sens. 12 (13). https://doi.org/10.3390/rs12132102.

Katiraie-Boroujerdy, P.S., Nasrollahi, N., Hsu, K. lin, Sorooshian, S., 2016. Quantifying the reliability of four global datasets for drought monitoring over a semiarid region. Theor. Appl. Climatol. 123 (1–2), 387–398. https://doi.org/10.1007/s00704-014-1360-3.

Kawo, N.S., Hordofa, A.T., Karuppannan, S., 2021. Performance evaluation of GPM-IMERG early and late rainfall estimates over Lake Hawassa catchment, Rift Valley Basin, Ethiopia. Arab. J. Geosci. 14 (4), 1–14. https://doi.org/10.1007/s12517-021-06599-1.
Kidd, C., Kniveton, D.R., Todd, M.C., Bellerby, T.J., 2003. Satellite rainfall estimation using combined passive microwave and infrared algorithms. J. Hydrometeorol. 4 (6), 1088–1104. https://doi.org/10.1175/1525-7541(2003)004< 1088:SREUCP> 2.0.CO;2.
Korecha, D., Barnston, A.G., 2007. Predictability of June-September rainfall in Ethiopia. Mon. Weather Rev. 135 (2), 628–650. https://doi.org/10.1175/MWR3304.1.
Korecha, D., Sorteberg, A., 2013. Validation of operational seasonal rainfall forecast in Ethiopia. Water Resour. Res. 49 (11), 7681–7697. https://doi.org/10.1002/2013WR013760.
Kottek, M., Grieser, J., Beck, C., Rudolf, B., Rubel, F., 2006. World map of the Köppen-Geiger climate classification updated. Meteorol. Z. 15 (3), 259–263. https://doi.org/10.1127/0941-2948/2006/0130.
Kuligowski, R.J., 2002. A self-calibrating real-time GOES rainfall algorithm for short-term rainfall estimates. J. Hydrometeorol. 3 (2), 112–130. https://doi.org/10.1175/1525-7541(2002)003< 0112:ASCRTG> 2.0.CO;2.
Kuligowski, R.J., Li, Y., Hao, Y., Zhang, Y., 2016. Improvements to the GOES-R rainfall rate algorithm. J. Hydrometeorol. 17 (6), 1693–1704. https://doi.org/10.1175/JHM-D-15-0186.1.
Kumar, L.S., 2021. Calculation and analysis of cloud attenuation and other cloud parameters in India for earth-space links. Adv. Space Res. 68 (10), 3957–3970. https://doi.org/10.1016/j.asr.2021.07.028.
Lakew, H.B., Moges, S.A., Asfaw, D.H., 2020a. Hydrological performance evaluation of multiple satellite precipitation products in the upper Blue Nile basin, Ethiopia. J. Hydrol.: Reg. Stud. 27 (August 2018), 100664. https://doi.org/10.1016/j.ejrh.2020.100664.
Lehner, B., Grill, G., 2013. Global river hydrography and network routing: Baseline data and new approaches to study the world's large river systems. Hydrol. Process. 27 (15), 2171–2186. https://doi.org/10.1002/hyp.9740.
Lemma, E., Upadhyaya, S., Ramsankaran, R., 2022. Meteorological drought monitoring across the main river basins of Ethiopia using satellite rainfall product. Environ. Syst. Res. 11 (1). https://doi.org/10.1186/s40068-022-00251-x.
Liu, J., Xia, J., She, D., Li, L., Wang, Q., Zou, L., 2019. Evaluation of six satellite-based precipitation products and their ability for capturing characteristics of extreme precipitation events over a climate transition area in China. Remote Sens. 11 (12), 1–21. https://doi.org/10.3390/rs11121477.
Lober, C., Fayne, J., Hashemi, H., Smith, L.C., 2023. Bias correction of 20 years of IMERG satellite precipitation data over Canada and Alaska. J. Hydrol.: Reg. Stud. 47, 101386. https://doi.org/10.1016/j.ejrh.2023.101386.
Love, T.B., Kumar, V., Xie, P.P., Thiaw, W., 2004. A 20-year daily Africa precipitation climatology using satellite and gauge data. Bull. Am. Meteorol. Soc. 5213–5216.
Macharia, D., Fankhauser, K., Selker, J.S., Neff, J.C., Thomas, E.A., 2022. Validation and Intercomparison of Satellite-Based Rainfall Products over Africa with TAHMO In Situ Rainfall Observations. J. Hydrometeorol. 23 (7), 1131–1154. https://doi.org/10.1175/JHM-D-21-0161.1.
Maggioni, V., Massari, C., Kidd, C., 2021. Errors and uncertainties associated with quasiglobal satellite precipitation products. Precip. Sci.: Meas., Remote Sens., Microphys. Model. 377–390. https://doi.org/10.1016/B978-0-12-822973-6.00023-8.
Mahmoud, M.T., Mohammed, S.A., Hamouda, M.A., & Mohamed, M.M. (2021). *Impact of Topography and Rainfall Intensity on the Accuracy of IMERG Precipitation Estimates in an Arid Region.*
Maidment, R.I., Grimes, D., Allan, R.P., Tarnavsky, E., Marcstringer, M., Hewison, T., Roebeling, R., Black, E., 2014. The 30 year TAMSAT african rainfall climatology and time series (TARCAT) data set, 10,619-10,644 J. Geophys. Res. 119 (18). https://doi.org/10.1002/2014JD021927.
Maidment, R.I., Grimes, D., Black, E., Tarnavsky, E., Young, M., Greatrex, H., Allan, R.P., Stein, T., Nkonde, E., Senkunda, S., Alcántara, E.M.U., 2017. A new, long-term daily satellite-based rainfall dataset for operational monitoring in Africa. Sci. Data 4. https://doi.org/10.1038/sdata.2017.63.
Massari, C., Brocca, L., Pellarin, T., Abramowitz, G., Filippucci, P., Ciabatta, L., Maggioni, V., Kerr, Y., Fernandez Prieto, D., 2020. A daily 25 km short-latency rainfall product for data-scarce regions based on the integration of the Global Precipitation Measurement mission rainfall and multiple-satellite soil moisture products. Hydrol. Earth Syst. Sci. 24 (5), 2687–2710. https://doi.org/10.5194/hess-24-2687-2020.
Matingo, T., Gumindoga, W., & Makurira, H. (2018). Evaluation of sub daily satellite rainfall estimates through flash flood modelling in the Lower Middle Zambezi Basin. 59–65.
McRoberts, D.B., Nielsen-Gammon, J.W., 2017. Detecting beam blockage in radar-based precipitation estimates. J. Atmos. Ocean. Technol. 34 (7), 1407–1422. https://doi.org/10.1175/JTECH-D-16-0174.1.
Mekonnen, K., Melesse, A.M., Woldesenbet, T.A., 2021. Spatial evaluation of satellite-retrieved extreme rainfall rates in the Upper Awash River Basin, Ethiopia. Atmos. Res. 249, 105297. https://doi.org/10.1016/j.atmosres.2020.105297.
Mekonnen, K., Melesse, A.M., Woldesenbet, T.A., 2022. How suitable are satellite rainfall estimates in simulating high flows and actual evapotranspiration in MelkaKunitre catchment, Upper Awash Basin, Ethiopia? Sci. Total Environ. 806. https://doi.org/10.1016/j.scitotenv.2021.150443.
Mekonnen, K., Velpuri, N.M., Leh, M., Akpoti, K., Owusu, A., Tinonetsana, P., Hamouda, T., Ghansah, B., Paranamana, T.P., Munzimi, Y., 2023. Accuracy of satellite and reanalysis rainfall estimates over Africa: A multi-scale assessment of eight products for continental applications. J. Hydrol.: Reg. Stud. 49 (April), 101514. https://doi.org/10.1016/j.ejrh.2023.101514.
Mera, G.A., 2018. Drought and its impacts in Ethiopia. Weather Clim. Extrem. 22 (ember 2017), 24–35. https://doi.org/10.1016/j.wace.2018.10.002.
Mohammed, S., Hamouda, M., Mahmoud, M., & Mohamed, M. (2020). Performance of GPM-IMERG precipitation products under diverse topographical features and multiple-intensity rainfall in an arid region. Hydrology and Earth System Sciences Discussions, January, 1–27.
de Moraes Cordeiro, A.L., Blanco, C.J.C., 2021. Assessment of satellite products for filling rainfall data gaps in the Amazon region. Nat. Resour. Model. 34 (2). https://doi.org/10.1111/nrm.12298.
Mosaffa, H., Filippucci, P., Massari, C., Ciabatta, L., Brocca, L., 2023. SM2RAIN-Climate, a monthly global long-term rainfall dataset for climatological studies. Sci. Data 10 (1), 1–14. https://doi.org/10.1038/s41597-023-02654-6.
Moura, G., Filho, R., Hugo, V., Coelho, R., Freitas, S., Xuan, Y., & Brocca, L. (2022). Jo ur na of. In Atmospheric Research. Atmospheric Research. https://doi.org/10.1016/j.atmosres.2022.106259.
NASA Shuttle Radar Topography Mission (SRTM). (2013). Shuttle Radar Topography Mission (SRTM) Global. Distributed by OpenTopography. https://doi.org/10.5069/G9445JDF. Accessed: 2024-01-22.
Nashwan, M.S., Shahid, S., Dewan, A., Ismail, T., Alias, N., 2020. Performance of five high resolution satellite-based precipitation products in arid region of Egypt: An evaluation. Atmos. Res. 236 (October 2019), 104809. https://doi.org/10.1016/j.atmosres.2019.104809.
Nguyen, P., Ombadi, M., Sorooshian, S., Hsu, K., AghaKouchak, A., Braithwaite, D., Ashouri, H., Rose Thorstensen, A., 2018. The PERSIANN family of global satellite precipitation data: A review and evaluation of products. Hydrol. Earth Syst. Sci. 22 (11), 5801–5816. https://doi.org/10.5194/hess-22-5801-2018.
Nicholson, S.E., 2017. Climate and climatic variability of rainfall over eastern Africa. Rev. Geophys. 55 (3), 590–635. https://doi.org/10.1002/2016RG000544.
Nile, B., Bayissa, Y., 2017. Eval. Satell. -Based Rainfall Estim. Appl. Monit. Meteorol. Drought 1–17. https://doi.org/10.3390/rs9070669.
NMA, N.M.A. (2015). Guide to the use of weather and Climate Information (WCI) for agricultural practices over selected districts of Tigray, Ethiopia. February, 78. ⟨https://www.google.com/url?sa=t&rct=j&q= &esrc=s&source=web&cd= 3&ved= 2ahUKEwisgPTClqjfAhUOTn0KHT6HAc0QFjACegQIAhAC&url=http%3A%2F%2Fwww.wmo.int%2Fpages%2Fprog%2Fdra%2Fraf%2Fdocuments%2FClimat%2520Guide%2520for%2520Tigray%2520and%2520SNNPR.pdf&usg=AOvVaw2p⟩.
Ogbu, K.N., Hounguè, N.R., Gbode, I.E., Tischbein, B., 2020. Performance evaluation of satellite-based rainfall products over Nigeria. Climate 8 (10), 1–23. https://doi.org/10.3390/cli8100103.
Omondi, C.K., Rientjes, T.H.M., Booij, M.J., Nelson, A.D., 2021. Satellite rainfall bias assessment for crop growth simulation – A case study of maize growth in Kenya. Agric. Water Manag. 258 (October). https://doi.org/10.1016/j.agwat.2021.107204.
Palharini, R.S.A., Vila, D.A., Rodrigues, D.T., Quispe, D.P., Palharini, R.C., de Siqueira, R.A., de Sousa Afonso, J.M., 2020. Assessment of the extreme precipitation by satellite estimates over South America. Remote Sens. 12 (13), 1–23. https://doi.org/10.3390/rs12132085.
Park, N.W., Kyriakidis, P.C., Hong, S., 2017. Geostatistical integration of coarse resolution satellite precipitation products and rain gauge data to map precipitation at fine spatial resolutions. Remote Sens. 9 (3), 1–19. https://doi.org/10.3390/rs9030255.

Prakoso, W.G., Murtilaksono, K., Tarigan, S.D., Purwanto, Y.J., 2018. Hydrological similarity approach and rainfall satellite utilization for mini hydro power dam basic design (case study on the ungauged catchment at West Borneo, Indonesia). IOP Conf. Ser.: Earth Environ. Sci. 149 (1). https://doi.org/10.1088/1755-1315/149/1/012039.

Qureshi, S., Koohpayma, J., Firozjaei, M.K., Kakroodi, A.A., 2022. Evaluation of seasonal, drought, and wet condition effects on performance of satellite-based precipitation data over different climatic conditions in Iran. Remote Sens. 14 (1). https://doi.org/10.3390/rs14010076.

Rahmawati, N., Lubczynski, M.W., 2018. Validation of satellite daily rainfall estimates in complex terrain of Bali Island, Indonesia. Theor. Appl. Climatol. 134 (1–2), 513–532. https://doi.org/10.1007/s00704-017-2290-7.

Romilly, T.G., Gebremichael, M., 2011b. Evaluation of satellite rainfall estimates over Ethiopian river basins. Hydrol. Earth Syst. Sci. 15 (5), 1505–1514. https://doi.org/10.5194/hess-15-1505-2011.

Romilly, T.G., Gebremichael, M., 2011a. Evaluation of satellite rainfall estimates over Ethiopian river basins, 2008, 1505–1514. https://doi.org/10.5194/hess-15-1505-2011.

Sarkar, M., Bailey, A., Blossey, P., De Szoeke, S.P., Noone, D., Quiñones Meléndez, E., Leandro, M.D., Chuang, P.Y., 2023. Sub-cloud rain evaporation in the North Atlantic winter trade winds derived by pairing isotopic data with a bin-resolved microphysical model. Atmos. Chem. Phys. 23 (19), 12671–12690. https://doi.org/10.5194/acp-23-12671-2023.

Satgé, F., Ruelland, D., Bonnet, M.P., Molina, J., Pillco, R., 2019. Consistency of satellite-based precipitation products in space and over time compared with gauge observations and snow- hydrological modelling in the Lake Titicaca region. Hydrol. Earth Syst. Sci. 23 (1), 595–619. https://doi.org/10.5194/hess-23-595-2019.

Schutgens, N., Tsyro, S., Gryspeerdt, E., Goto, D., Weigum, N., Schulz, M., Stier, P., 2017. On the spatio-temporal representativeness of observations. Atmos. Chem. Phys. 17 (16), 9761–9780. https://doi.org/10.5194/acp-17-9761-2017.

Shaowei, N., Jie, W., Juliang, J., Xiaoyan, X., Yuliang, Z., Fan, S., Linlin, Z., 2022. Comprehensive evaluation of satellite-derived precipitation products considering spatial distribution difference of daily precipitation over eastern China. J. Hydrol.: Reg. Stud. 44 (May), 101242. https://doi.org/10.1016/j.ejrh.2022.101242.

Sheffield, J., Wood, E.F., Pan, M., Beck, H., Coccia, G., Serrat-Capdevila, A., Verbist, K., 2018. Satellite Remote Sensing for Water Resources Management: Potential for Supporting Sustainable Development in Data-Poor Regions. Water Resour. Res. 54 (12), 9724–9758. https://doi.org/10.1029/2017WR022437.

Siddig, M.S.A., Ibrahim, S., Yu, Q., Abdalla, A., Osman, Y., Atiem, I.A., Hamukwaya, S.L., Taha, M.M.M., 2022. Bias Adjustment of Four Satellite-Based Rainfall Products Using Ground-Based Measurements over Sudan. Water (Switz.) 14 (9), 1–20. https://doi.org/10.3390/w14091475.

Tadesse, K.E., Melesse, A.M., Abebe, A., Lakew, H.B., Paron, P., 2022. Evaluation of Global Precipitation Products over Wabi Shebelle River Basin, Ethiopia. Hydrology 9 (5), 1–17. https://doi.org/10.3390/hydrology9050066.

TAMSAT Group. (2016). Draft TAMSAT Technical Report: TAMSAT version 3 calibration methodology. September. ⟨http://www.met.reading.ac.uk/~emily/TAMSAT_technical_report.pdf⟩.

Tang, X., Li, H., Qin, G., Huang, Y., Qi, Y., 2023. Evaluation of Satellite-Based Precipitation Products over Complex Topography in Mountainous Southwestern China. Remote Sens. 15 (2). https://doi.org/10.3390/rs15020473.

Tapiador, F.J., Marcos, C., Navarro, A., Jiménez-Alcázar, A., Galdón, R.M., Sanz, J., 2018. Decorrelation of satellite precipitation estimates in space and time. Remote Sens. 10 (5). https://doi.org/10.3390/rs10050752.

Taye, M., Mengistu, D., Sahlu, D., 2023. Performance evaluation of multiple satellite rainfall data sets in central highlands of Abbay Basin, Ethiopia. Eur. J. Remote Sens. 56 (1). https://doi.org/10.1080/22797254.2023.2233686.

Taye, M., Sahlu, D., Zaitchik, B.F., Neka, M., 2020. Evaluation of satellite rainfall estimates for meteorological drought analysis over the upper blue nile basin, Ethiopia. Geosci. (Switz.) 10 (9), 1–22. https://doi.org/10.3390/geosciences10090352.

Teixeira de Aguiar, J., Lobo, M., 2020. Reliability and discrepancies of rainfall and temperatures from remote sensing and Brazilian ground weather stations. Remote Sens. Appl.: Soc. Environ. 18 (March), 100301. https://doi.org/10.1016/j.rsase.2020.100301.

Thakur, M.K., Kumar, T.V.L., Koteswara Rao, K., Barbosa, H., Rao, V.B., 2019. A new perspective in understanding rainfall from satellites over a complex topographic region of India. Sci. Rep. 9 (1), 1–10. https://doi.org/10.1038/s41598-019-52075-y.

Thiemig, V., Rojas, R., Zambrano-Bigiarini, M., De Roo, A., 2013. Hydrological evaluation of satellite-based rainfall estimates over the Volta and Baro-Akobo Basin. J. Hydrol. 499, 324–338. https://doi.org/10.1016/j.jhydrol.2013.07.012.

Toté, C., Patricio, D., Boogaard, H., van der Wijngaart, R., Tarnavsky, E., Funk, C., 2015. Evaluation of satellite rainfall estimates for drought and flood monitoring in Mozambique. Remote Sens. 7 (2), 1758–1776. https://doi.org/10.3390/rs70201758.

Upadhyaya, S., Ramsankaran, R.A.A.J., 2016. Modified-INSAT Multi-Spectral Rainfall Algorithm (M-IMSRA) at climate region scale: Development and validation. Remote Sens. Environ. 187, 186–201. https://doi.org/10.1016/j.rse.2016.10.013.

Velpuri, N.M., Pervez, M.S., Cushing, W.M., 2016. A Multisource Satellite Data and Hydrologic Modeling Approach. Hydropower Assess. Boliv. 65.

Vergara, H., Hong, Y., Gourley, J.J., Anagnostou, E.N., Maggioni, V., Stampoulis, D., Kirstetter, P.E., 2014. Effects of resolution of satellite-based rainfall estimates on hydrologic modeling: Skill at different scales. J. Hydrometeorol. 15 (2), 593–613. https://doi.org/10.1175/JHM-D-12-0113.1.

Vivekanandan, J., Yates, D.N., Brandes, E.A., 1999. The influence of terrain on rainfall estimates from radar reflectivity and specific propagation phase observations. J. Atmos. Ocean. Technol. 16 (7), 837–845. https://doi.org/10.1175/1520-0426(1999)016< 0837:TIOTOR> 2.0.CO;2.

Wang, W., Hocke, K., Mätzler, C., 2021. Physical retrieval of rain rate from ground-based microwave radiometry. Remote Sens. 13 (11). https://doi.org/10.3390/rs13112217.

Wang, F., Yang, H., Wang, Z., Zhang, Z., Li, Z., 2019. Drought evaluation with CMORPH satellite precipitation data in the Yellow River basin by using Gridded Standardized Precipitation Evapotranspiration Index. Remote Sens. 11 (5), 1–19. https://doi.org/10.3390/rs11050485.

Wang, G., Zhang, P., Liang, L., Zhang, S., 2017. Evaluation of precipitation from CMORPH, GPCP-2, TRMM 3B43, GPCC, and ITPCAS with ground-based measurements in the Qinling-Daba Mountains, China. PLoS ONE 12 (10), 1–23. https://doi.org/10.1371/journal.pone.0185147.

WBG. (2020). Climate Risk Profile: Ethiopia (2020): The World Bank Group. 24.

Wei, C., Dong, X., Ma, Y., Gou, J., Li, L., Bo, H., Yu, D., Su, B., 2023. Applicability comparison of various precipitation products of long-term hydrological simulations and their impact on parameter sensitivity. J. Hydrol. 618 (January). https://doi.org/10.1016/j.jhydrol.2023.129187.

WMO. (2012). Atlas of Mortality and Economic Losses From Weather, Climate and Water Extremes (Issue 1123).

Xia, L., Zhao, F., Mao, K., Yuan, Z., Zuo, Z., Xu, T., 2018. SPI-based analyses of drought changes over the past 60 years in China'S major crop-growing areas. Remote Sens. 10 (2), 1–15. https://doi.org/10.3390/rs10020171.

Xiang Soo, E.Z., Wan Jaafar, W.Z., Lai, S.H., Othman, F., Elshafie, A., Islam, T., Srivastava, P., Othman Hadi, H.S., 2020. Evaluation of bias-adjusted satellite precipitation estimations for extreme flood events in Langat river basin, Malaysia. Hydrol. Res. 51 (1), 105–126. https://doi.org/10.2166/nh.2019.071.

Yalew, A.W., 2022. The Ethiopian energy sector and its implications for the SDGs and modeling. Renew. Sustain. Energy Transit. 2 (February), 100018. https://doi.org/10.1016/j.rset.2022.100018.

Yoshimot, S., Amarnath, G., 2017. Applications of satellite-based rainfall estimates in flood inundation modeling-A case study in Mundeni Aru River Basin, Sri Lanka. Remote Sens. 9 (10). https://doi.org/10.3390/rs9100998.

Young, M.P., Williams, C.J.R., Christine Chiu, J., Maidment, R.I., Chen, S.H., 2014. Investigation of discrepancies in satellite rainfall estimates over Ethiopia. J. Hydrometeorol. 15 (6), 2347–2369. https://doi.org/10.1175/JHM-D-13-0111.1.

Zambrano-bigiarini, M., Nauditt, A., Birkel, C., Verbist, K., Ribbe, L., 2017. Tempo Spat. Eval. Satell. -Based Rainfall Estim. Across Complex Topogr. Clim. gradients Chile 1295–1320. https://doi.org/10.5194/hess-21-1295-2017.